

AD-A069 041

TEXAS UNIV AT EL PASO DEPT OF ELECTRICAL ENGINEERING  
ATMOSPHERIC TRANSMITTANCE STUDY WITH THE METEOROLOGICAL SATELLI--ETC(U)  
OCT 76 R E BRUCE, J H PIERLUISSI, S K WEAVER DAEA18-76-C-0019  
PR4-76-DC-30-PT-2 NL

UNCLASSIFIED

1 OF 2  
AD  
AO-9041





**LEVEL**  
The University of Texas  
at El Paso

4069 042

**LEVEL**

AD A069041



DDC  
FORM  
MAY 29 1979  
C

DDC FILE COPY

# INSTRUMENTATION AND MEASUREMENT SYSTEMS

Graduate - Research Program

This document has been approved  
for public release and sale; its  
distribution is unlimited.

PHYSICS DEPARTMENT  
AND  
ELECTRICAL ENGINEERING DEPARTMENT

79 05 24 050



Pages cut  
off Within  
Doc'

---

## **DISCLAIMER NOTICE**

**THIS DOCUMENT IS BEST QUALITY  
PRACTICABLE. THE COPY FURNISHED  
TO DDC CONTAINED A SIGNIFICANT  
NUMBER OF PAGES WHICH DO NOT  
REPRODUCE LEGIBLY.**

6

1

Atmospheric Transmittance Study with  
the Meteorological Satellite Technical  
Area at White Sands Missile Range.

Part II.

STUDIES RELATED TO THE INVERSION OF THE RADIATIVE  
TRANSFER EQUATION AND HIGH RESOLUTION  
TRANSMITTANCE CALCULATIONS.



PART II

CONTRACT

15 DAEA18-76-C-2019

9 FINAL REPORT.

10/31/76

14 PR4-76-DC-30 - PT-2

1 Oct 75-30 Sep 76

by

10

Rufus E. Bruce  
Joseph H. Pierluissi  
and  
Sandra K. Weaver

11 31 Oct 76

12 10/4/76

Prepared for:

United States Army Electronics Command  
Atmospheric Sciences Laboratory  
White Sands Missile Range  
New Mexico

Submitted by

Physics Department  
and

Electrical Engineering Department  
The University of Texas at El Paso  
El Paso, Texas

Rufus E. Bruce  
Joseph H. Pierluissi  
Project Directors

This document has been approved  
for public release and sale; its  
distribution is unlimited.

408 579

LB



REPORT DOCUMENTATION PAGE		READ INSTRUCTIONS BEFORE COMPLETING FORM
1. REPORT NUMBER PR4-76-DC-30	2. GOVT ACCESSION NO.	3. RECIPIENT'S CATALOG NUMBER
4. TITLE (and Subtitle) Studies Related to the Inversion of the Radiative Transfer Equation and High Resolution Transmittance Calculations		5. TYPE OF REPORT & PERIOD COVERED Final Report Oct. 1, 1975 Part II Sept. 30, 1976
7. AUTHOR(s) Rufus E. Bruce Joseph H. Pierluissi Sandra K. Weaver		6. PERFORMING ORG. REPORT NUMBER
9. PERFORMING ORGANIZATION NAME AND ADDRESS Physics and Electrical Engineering Depts. The University of Texas at El Paso El Paso, Texas 79968		8. CONTRACT OR GRANT NUMBER(s) DAEA18-76-C-0019
11. CONTROLLING OFFICE NAME AND ADDRESS United States Army Electronics Command Atmospheric Sciences Laboratory White Sands Missile Range, New Mexico 88002		10. PROGRAM ELEMENT, PROJECT, TASK AREA & WORK UNIT NUMBERS
14. MONITORING AGENCY NAME & ADDRESS (if different from Controlling Office)		12. REPORT DATE October 31, 1976
		13. NUMBER OF PAGES 98
		15. SECURITY CLASS. (of this report) Unclassified
		15a. DECLASSIFICATION/DOWNGRADING SCHEDULE
16. DISTRIBUTION STATEMENT (of this Report) Approved for Public Release: Distribution Unlimited		
17. DISTRIBUTION STATEMENT (of the abstract entered in Block 20, if different from Report)		
18. SUPPLEMENTARY NOTES Contracting Officer Technical Representative Richard B. Gomez Atmospheric Sciences Laboratory White Sands Missile Range New Mexico 88002		
19. KEY WORDS (Continue on reverse side if necessary and identify by block number) VTPR Soundings, SMS Cloud Data, Atmospheric Composition, Temperature Errors Transmittances		
20. ABSTRACT (Continue on reverse side if necessary and identify by block number) This report concerns 1) a method for combining SMS cloud data into VTPR retrievals; 2) the expected differences between radiosonde and VTPR temperature profiles; 3) CO <sub>2</sub> atmospheric composition inferred from radiance data and 4) homogeneous and slant path line-by-line transmittance studies. This portion of the final report covers requirements 3.2.4, 3.2.5, 3.2.6 and part of 3.2.3.		

## FOREWARD

This is Part II of the final report under Contract DAEA18-76-C-0019 entitled Atmospheric Transmittance Study with the Meteorological Satellite Technical Area of the Atmospheric Sciences Laboratory at *script 1* White Sands Missile Range. Part I contains a study and development of band models for use in connection with techniques for the calculation of atmospheric transmittance along slant-paths. Part II contains the report on the studies related to the inversion of the radiative transfer equation for temperature, composition and possible cloud correction in the  $15\mu\text{ CO}_2$  band region. Also included there is a discussion of the method used in this study for the calculation of atmospheric transmittance using line spectral parameters. Part III deals with the study of SMS digital data and their use in severe storm and cloud studies.

ADDRESS TO:	White Sands	<input checked="checked" type="checkbox"/>
TO:	Ball Station	<input type="checkbox"/>
FROM:		
DATE:		
BY		
DISTRIBUTION/AVAILABILITY CODES		
		SPECIAL
A	23	CT

## TABLE OF CONTENTS

1. Studies Related to the Inversion of the Radiative Transfer Equations: VTPR Soundings and Atmospheric Composition	1
1.1 General Statement of Direction of Studies	2
1.2 Studies on the Expected Difference Between Radiosonde Temperature Profiles and VTPR Sounded Temperature Profiles	5
1.2.1 Abstract	7
1.3 Optimized Study Using SMS Infrared Cloud Data in VTPR Temperature Soundings	10
1.3.1 Discussion	11
Table I	14
Table II	18
1.4 Composition Profile Studies	23
1.4.1 Summary	24
1.4.2 Perturbation Technical Results	25
1.4.3 Iteration Technique Results	29
1.4.4 Recommendations for Further Work	33
1.4.5 Bibliography	34
1.4.6 Figures	35
2. Studies and Calculations Relating to High Resolution Atmospheric Transmittance	56
2.1 Summary	57
2.2 Considerations in High Resolution Transmittances	60
2.2.1 Summary of Radiative Transfer Problem	61



TABLE OF CONTENTS CONTINUED

2.2.2	General Aspects of Transmittance Computation Techniques	63
2.2.3	Data Available for Calculations and Error Sources	65
2.2.4	Philosophy of Calculation Approach	66
2.3	Homogeneous Paths	67
2.4	Slant Paths	69
Appendix 1		72
Appendix 2		78
Appendix 3		85

1. STUDIES RELATED TO THE INVERSION OF THE RADIATIVE  
TRANSFER EQUATION: VTPR TEMPERATURE SOUNDINGS AND  
ATMOSPHERIC COMPOSITION

Contributors to the effort reported in this section  
were Toran Hostbjoer (Section 1.4) and N. Goravanchi  
(Section 1.3).

1.1 GENERAL STATEMENT OF DIRECTION OF STUDIES



This section reports on the contractual efforts under Requirements 3.2.5, 3.2.6 and part of 3.2.3. All of the sections relate to probable errors in VTPR sounded temperature profiles and have in common the inversion of the radiative transfer equation. The underlying philosophy of our effort under this section is to develop techniques that will provide accurate VTPR temperature profiles under cloudy conditions over land masses. This requires techniques that will not only adequately correct for cloud conditions but will also compensate for atmospheric composition fluctuations.

Under requirement 3.2.6 we have undertaken (and completed except for checking for possible errors) a study to determine the improvement in VTPR temperature profiles if SMS infrared type cloud data were incorporated into the retrieval scheme. Our preliminary result indicates an improvement by at least a factor of 2 (higher altitude temperatures have greater improvement).

In either evaluating errors in VTPR temperatures or in evaluating possible errors in composition retrievals, one must know the relationship between a radiosonde temperature profile and an area average (VTPR) temperature profile. This evaluation (i.e. the determination of the extensiveness of temperature differences for an error to exist) is basic to the evaluation of possible errors. This study, in two parts, is almost complete. It is reported on in section 1.2.

Efforts to evaluate VTPR temperature errors resulting from probable atmospheric composition errors, 3.2.3, have been directed toward the evaluation of possible CO<sub>2</sub> fluctuations. The approach has been to combine

this study with the effort under 3.2.5 to obtain evidence, if any, of  $\text{CO}_2$  deviations. This could then be combined with a previous study (see Appendix) to evaluate probable errors. The preliminary result of effort 3.2.5 is that there is a variation of the high altitude  $\text{CO}_2$  content. The result cannot be applied to lower altitudes because we did not have infrared cloud data for the times coincident with the inverted VTPR data. The result of this general study is reported in section 1.4.

In summary, the results of these studies indicate:

1. Radiometrically derived  $\text{CO}_2$  atmospheric content at high altitudes (25 km) is less than 320 ppm during daylight hours.
2. The radiometric technique can be used to determine atmospheric  $\text{H}_2\text{O}$  vapor content, provided the cloud problem can be solved.
3. If SMS infrared data can be combined into VTPR retrieval techniques substantial reductions in temperature errors will result.

The major direction of future work under these and related efforts should be directed toward:

1. Incorporating (and evaluating) cloud corrections in a watervapor determination program. This program should be based upon the  $\text{CO}_2$  iterative technique.
2. Devising an adequate  $\text{CO}_2$  transmittance model (preferably a Smith Polynomial of at least 2nd or 3rd order in composition) for use in the  $\text{CO}_2$  retrieval effort. The cloud correction scheme used for  $\text{H}_2\text{O}$  should be used in this effort.
3. Examine the possibility of incorporating the above two studies into the VTPR retrieval techniques.

1.2 STUDIES ON THE EXPECTED DIFFERENCES BETWEEN RADIOSONDE  
TEMPERATURE PROFILES AND VTPR SOUNDED TEMPERATURE PROFILES



One of the difficulties in evaluating the accuracy of radiometrically determined temperature profiles is the uncertainty in their relationship with radiosonde measurements made in or near the viewed region. This difficulty is further complicated if the radiosonde measurement is temporally displaced.

A study was made of this problem utilizing radiosonde data collected at WSMR between January 1969 and June 1970. The results of the first phase of the study (expected difference between simultaneous, but spatially separated, radiosonde and radiometric temperature profiles) was reported to the American Geophysical Union in December 1975. An open literature article reporting these results has been submitted for publication. A copy of the abstract of the report follows this section.

The second phase of the study is nearing completion. This phase of the study concerns the expected difference between a spatially and temporally displaced radiosonde temperature measurement and a VTPR temperature sounding. The computer program has been written and tested for this part of the study. A preliminary result indicates that the temperature errors resulting from time displacements may be represented by a linear relationship with a larger intercept but small slope (i.e., a large error for small time shifts that does not increase appreciably with moderate time increases - up to three hours).

This second phase should be completed by November and a written report will be submitted by December or January.

1.2.1 ABSTRACT

EXPERIMENTAL STUDY OF THE RELATIONSHIP BETWEEN  
RADIOSONDE TEMPERATURES AND RADIOMETRIC-AREA TEMPERATURES

by

Rufus E. Bruce  
University of Texas at El Paso  
El Paso, Texas

Louis D. Duncan  
Atmospheric Sciences Laboratory  
US Army Electronics Command  
White Sands Missile Range, New Mexico

Joseph H. Pierluissi  
University of Texas at El Paso  
El Paso, Texas

# ABSTRACT

A large sample of temperature observations was statistically analyzed to estimate horizontal temperature variability as a function of distance. These estimates were determined at several altitudes from the surface to 15 km and are applicable to horizontal distances up to 175 km.

The results were used to assess the amount of disagreement one should expect when comparing radiosonde temperature measurements with corresponding measurements derived from satellite radiometric observations. The conclusion was that horizontal temperature variations over the radiometrically observed area contribute approximately 1K root mean square (rms) disagreement between such comparisons. When the separation distance between the radiosonde and satellite observation approaches 200 km, rms differences of greater than 2K are to be expected.



1.3 OPTIMIZED STUDY OF USING SMS INFRARED CLOUD  
DATA IN VTPR TEMPERATURE SOUNDINGS

### 1.3.1 Discussion

This study has been undertaken to determine the extent of possible improvements in VTPR temperature soundings if SMS infrared cloud data were utilized in the inversion programs. It is motivated by the fact that the SMS data presently contains the cloud data needed for the VTPR retrievals and secondarily that a VTPR instrument may some day be included on the geostationary satellites. Explicit in the study are the assumptions that automatic computer processes will be devised for the SMS data that will solve the registration problem and provide the necessary cloud data for the VTPR retrieval.

It is assumed that the basic raw data available from the SMS infrared processing will be an average percent cloud cover and an average cloud top temperature for each VTPR viewed spot. No attempt has been made in this preliminary study to evaluate the slant path effect on determining cloud percentages and cloud top temperatures nor has any attempt been made to evaluate differences in the effective cloud top temperatures for the two instruments. Grey scale registration for the SMS data also has not been considered. These problems are suggested as possible extensions of the present work.

In order to examine the possible improvements, a synthetic study was undertaken. The Atmospheric Sciences Laboratory temperature retrieval program, SATFA, was used to determine the temperature profile for each spot of a 7 X 7 VTPR array. Three different sets of meteorologically consistent cloud top temperatures and cloud cover percentages for each spot of the 7 X 7 array were generated. The cloud top data, the temperature profiles and an assumed watervapor profile (not consistent with the cloud data) were used to compute synthetic radiances for the VTPR.

The single watervapor profile, the radiances, the cloud percentages and the cloud temperatures for each spot were used as input in a modified retrieval program. In this modified program clear channel radiances were not computed. The only modification made was in the computation of trial radiances in the iterative scheme; weighting function were not modified. The trial radiances were computed by numerically integrating the transfer equation in two parts: the sum for pressure levels above the cloud top was left unmodified; the sum below the cloud top was modified by the factor  $(100 - \text{Cloud Percentage})/100$ . The cloud height pressure was determined each cycle using the latest computed temperature profile. The modified subroutine TNVERT of program SATFA is shown in Table I.

#### Results:

The temperatures retrieved using the above technique were compared to the actual temperatures used in the radiance calculations. Typically the RMS temperature difference for pressure levels above 300 mb was less than  $1^{\circ}\text{K}$ . RMS temperature differences for the entire profile were typically in the range  $1.6^{\circ}\text{K}$ . to  $1.8^{\circ}\text{K}$ .

A comparison was made of the retrieved temperature from the new scheme with those determined using program SATFA. The RMS temperature errors in the new scheme were substantially (approximately 1/2) smaller than the RMS temperature errors using program SATFA. A typical computer output for this comparison is shown in Table II.



The comparison with program SATFA indicated a possible error in the study. Examination of the SATFA result indicated errors upward toward  $5^{\circ}\text{K}$ . and in some cases even greater. The "SATFA" RMS profile errors were between  $3^{\circ}\text{K}$ . and  $4^{\circ}\text{K}$ . The author feels that these errors are excessive and error search has been undertaken. As of this writing no apparent error has been uncovered; however, all data is being rerun since it is the subject of the latter author's thesis. Upon completion of the rerun, a special report documenting the results will be prepared.

Even though an error is suspected, we do not believe that the general character of the result is wrong. The revised technique produces exceptionally small temperature error for altitudes greater than 300 mb. This result should not change. While lower altitude retrieved temperatures contain less error, the improvement is less dramatic.

TABLE I

TABLE I

```

300 SUBROUTINE INVERT (R,T,TD, K1,K2,IX)
301 DIMENSION R(100,3), T(3), P(3), RADD(3), T(100), TD(100)
302 COMMON /ZM12/ ZEM(49),ALPHA,RAD1(R,49),RCLD(3),A(100,8,1),TOUT(R
1),TSC,11
303 COMMON /ZG11/ IYPER
304 COMMON /ZG11NZ/ W(100,8),AV(100,6),CX1(49),P1(49)
305 COMMON /ZAL1/ P(100),T1(100),NO,NC,TH20(100,8),XNZ(8),TOWATP
306 COMMON /ZMT1NZ/ IAPP,DELTA,IPC,NPASS
307 COMMON /ZPSZ/ PSF,Z(100),XNU(3),C1,C2
308 COMMON /ZCC2/ IPC,IORN
309 N=C
C INITIALIZE WORKING T AND R ARRAYS
C
310 DO 10 I=1,NO
311 T(I)=T0(I)
312 DO 10 J=1,3
313 R(I,J)=A(I,1,K1)
314 DO 11 I=NO,00
315 11 T(I+1)=T(I)
316 DO 1111 J=1,3
317 DO 1111 I=NO,00
318 A(I+1,J,K1)=A(I,J,K1)
319 1111 R(I+1,J)=R(I,J)
320 DO 111 J=1,00
321 I=(99-J)+1
322 IF(T(I).GE.P1(IX).AND.P1(IX).GE.T(I-1)) GO TO 121
323 111 CONTINUE
324 121 NO1=I
C
C COMPUTE RADIANCE FOR INPUT PROFILE
325 DO 20 J=1,NC
326 RADD(J)=0.
327 DO 20 I=1,NO1
328 20 RADD(J)=RADD(J)+R(I,J)*W(I,J)
329 CC1=1.0-CX1(IX)
330 NO11=NO1+1
331 DO 78 I=NO11,NO
332 DO 78 J=1,6
333 78 RADD(J)=RADD(J)+CC1*R(I,J)*W(I,J)
334 WRITE(6,211) RADD
C BEGINNING OF ITERATION LOOP
335 30 N=N+1
336 DO 40 J=1,NC
337 R1(J)=R(J)/RADD(J)
338 40 IF(IYPER.GT.1) R1(J)=R(J)-RADD(J)
339 IF(IAPP.EQ.0) GO TO 80
340 DO 60 I=1,NO
341 SUM=0.
342 DO 50 J=1,NC
343 X=R1(J)-R(I,J)
344 IF(IYPER.GT.1) X=R1(J)
345 50 SUM=SUM+C2*XNU(J)/ALOG(C1*XNU(J)**3/X+1)*AV(I,J)
346 60 T(I)=SUM
347 DO 70 J=1,NC
348 RADD(J)=0.
349 DO 70 I=1,NO1
350 R(I,J)=C1*XNU(J)**3/(EXP(C2*XNU(J)/T(I))-1.)
351 70 RADD(J)=RADD(J)+R(I,J)*W(I,J)
352 CC1=1.0-CX1(IX)
353 NO11=NO1+1
354 DO 73 I=NO11,NO
355 DO 73 J=1,6
356 73 RADD(J)=RADD(J)+CC1*R(I,J)*W(I,J)
357 DO 22 I=1,NO
358 T(I)=T0(I)
359 DO 22 J=1,3
360 22 R(I,J)=A(I,J,K1)
361 DO 23 I=NO,00

```



```

362 23 T(I+1)=T(I)
363 DO 222 J=1,50
364 I=(50-J)+1
365 IF (T(I).GE.P1(IX).AND.P1(IX).GE.T(I-1)) GO TO 221
366 222 CONTINUE
367 221 N11=I
368 GO TO 170
C STATEMENTS 100 - 125 FOR APPROX CALCULATIONS
369 80 DO 110 I=1,N0
370 DB=0.
371 DO 90 J=1,NC
372 IF (ITYDBP.EQ.1) XX=(P1(J)-1.)*P(I,J)
373 IF (ITYDBP.GT.1) XX=P1(J)
374 90 DB=P1+XX+AV(I,J)
375 DO 100 J=1,NC
376 100 R(I,J)=R(I,J)+DB
377 110 T(I)=T(I)+DB/(.01*T(I)-1.3)
378 DO 120 J=1,NC
379 RADD(J)=0.
380 DO 120 I=1,N01
381 120 RADD(J)=RADD(J)+R(I,J)*W(I,J)
382 CC1=1.0-CX1(IX)
383 N011=N01+1
384 DO 70 I=N011,N0
385 DO 70 J=1,5
386 70 RADD(J)=RADD(J)+CC1*R(I,J)*W(I,J)
C CHECK FOR CONVERGENCE, OUTPUT, ETC
387 130 IO=0
388 IF (N.LT.NPASS) GO TO 140
389 IO=1
390 GO TO 170
391 140 IC=0
392 DO 150 J=1,NC
393 150 IF (ABS(R(J)-RADD(J)).GT.DELTA) IC=1
394 IF (IC.NE.0) GO TO 160
395 IO=1
396 GO TO 170
397 160 IF (IO.EQ.0) GO TO 30
C BEGIN OUTPUT SECTION
398 170 CONTINUE
399 WRITE (6,220) P,N,RADD
400 WRITE (6,230)
401 PP=P(N0)
402 P(N0)=PPF
403 P(N0)=PP
404 DO 190 I=1,50
405 D1=T(I)-T(I)
406 D2=T(I+50)-T(I+50)
407 TC1=T(I)-273.15
408 TC2=T(I+50)-273.15
409 190 WRITE (6,240) P(I),Z(I),T(I),T(I),D1,TC1,P(I+50),Z(I+50),T(
410 I,T(I+50),D2,TC2
411 NEW=0
412 IF (IO.EQ.0) GO TO 30
413 IF (NEW.EQ.2) GO TO 1000
414 DO 310 I=1,N0
415 SUM=0.
416 300 DO 300 J=1,NC
417 300 SUM=SUM+W(I,J)/P(J)
418 DO 310 J=1,NC

```

```

418      310  AV(I,J)=(W(I,J)/R(J))/SUM
419      IF(I*YPER.NE.7) GO TO 1000
420      DO 400 J=1,NO
421      SUM=0.
422      DO 410 I=1,NO
423      410  SUM=SUM+W(I,J)*W(I,J)
424      DO 400 I=1,NO
425      400  AV(I,J)=AV(I,J)+W(I,J)/SUM
426      1000 CONTINUE
427      IF(IORN.NO.1) GO TO 1001
428      GO TO 1002
429      1001 IF(NO.NO.100) GO TO 1005
430      NOX=NO+1
431      DO 1004 I=NOX,100
432      1004  T(I)=T(I-1)
433      1005 CONTINUE
434      WRITE(7,1003) (T(I),I=1,100)
435      1003 FORMAT(8F10.1)
436      1002 CONTINUE
437      RETURN
C
438      210  FORMAT (1H , 'ESTIMATED RADIANCE',11X,8F10.3)
439      220  FORMAT (1H , 'MEASURED RADIANCE',11X,8F10.3, ' COMPUTED RADIANCE PA
440      230  1SS NO ',13,8F10.3)
441      240  1  FORMAT (1H ,7X,'P          Z          TO          T          DIFF          ',21X,'P
442      2  7          TO          T          DIFF')
443      240  1  FORMAT(1H ,6F9.2,10X,6F9.2)
444      END

```

TABLE II



SUMMARY RESULTS FOR DATE, SEP. 8, 76 - LINE

SPEC 7

TABLE II

CLOUD TEMP		PI		CLOUD COVER		CX1											
277.000		0.050															
57.69 43.70		40.73 55.14		71.08 84.28		114.14 86.02		142 6.80		35.06		PC1=APC2=0107.					
PRESSURE		TRIAL		ACTUAL		ASL-MS		TEMP		NEW		TEMP					
LEVEL		TEMP		TEMP		TEMP		ERROR		TEMP		ERROR					
0.01	191.60	191.60	194.60	-2.70	192.10	-0.20											
0.02	204.70	205.00	208.10	-3.10	205.20	-0.30											
0.04	217.10	217.40	220.80	-3.40	217.70	-0.30											
0.08	228.00	228.40	232.10	-3.70	228.70	-0.30											
0.12	238.00	238.40	242.40	-4.00	238.70	-0.30											
0.15	247.10	247.50	251.50	-4.30	247.50	-0.40											
0.27	255.70	256.10	260.80	-4.70	256.50	-0.40											
0.33	263.40	263.90	268.70	-4.80	264.20	-0.40											
0.52	269.50	270.00	275.10	-5.10	270.40	-0.40											
0.69	269.50	270.00	275.10	-5.10	270.40	-0.40											
0.85	269.50	270.00	275.00	-5.00	270.40	-0.40											
1.14	269.50	270.00	275.00	-5.00	270.40	-0.40											
1.43	267.80	268.30	273.20	-4.90	268.70	-0.40											
1.77	263.90	264.40	269.10	-4.70	264.80	-0.40											
2.17	259.30	259.80	264.30	-4.50	260.10	-0.30											
2.63	255.20	255.70	259.90	-4.20	256.00	-0.30											
3.15	251.40	251.90	255.80	-3.90	252.10	-0.20											
3.74	248.50	249.00	252.60	-3.60	249.20	-0.20											
4.41	245.50	246.00	249.30	-3.30	246.10	-0.10											
5.16	242.90	243.50	246.30	-2.80	243.50	0.0											
5.99	240.50	241.10	243.80	-2.50	241.00	0.10											
6.92	238.00	238.60	240.70	-2.10	238.50	0.10											
7.95	235.00	235.60	237.40	-1.80	235.40	0.20											
9.08	232.20	232.80	234.30	-1.50	232.60	0.20											
10.32	229.10	229.70	231.40	-1.20	229.40	0.30											
11.67	221.70	222.30	223.30	-1.00	222.00	0.30											
13.15	220.40	221.00	221.90	-0.90	220.70	0.30											
14.76	219.10	219.70	220.40	-0.70	219.40	0.30											
16.50	217.90	218.50	219.00	-0.50	218.20	0.30											
18.39	216.70	217.30	217.60	-0.30	216.90	0.40											
20.43	215.90	216.50	216.60	-0.10	216.10	0.40											
22.62	216.20	216.80	216.80	0.0	216.40	0.40											
24.98	216.50	217.10	216.90	0.20	216.70	0.40											
27.50	216.70	217.30	216.80	0.50	216.90	0.40											
30.21	216.90	217.50	216.80	0.70	217.10	0.40											
33.09	215.70	216.30	215.40	0.90	215.80	0.50											
36.17	214.50	215.10	214.00	1.10	214.60	0.50											
39.45	213.30	213.80	212.60	1.20	213.40	0.40											
42.94	212.20	212.70	211.30	1.40	212.30	0.40											
46.64	211.00	211.50	210.00	1.50	211.10	0.40											
50.55	210.00	210.40	208.80	1.60	210.10	0.30											
54.72	209.50	209.90	208.10	1.80	209.60	0.30											
59.11	209.10	209.40	207.50	1.90	209.20	0.20											
63.75	208.60	208.90	206.80	2.10	208.70	0.20											
68.64	208.10	208.30	206.20	2.10	208.20	0.10											
73.80	208.10	208.20	206.00	2.20	208.20	0.0											
79.22	208.30	208.30	206.10	2.20	208.50	-0.20											
84.93	208.50	208.40	206.10	2.30	208.70	-0.10											
90.92	208.70	208.50	206.20	2.30	208.90	-0.40											
97.21	208.80	208.50	206.30	2.20	209.10	-0.60											

SUMMARY RESULTS FOR DATE, SEP. 8, 70-LINE

SPOT 7 contd

TABLE II contd.

CLCD TEMP PRESSURE LEVEL	FL TRIAL TEMP	CLCD COVER ACTUAL TEMP	CX1 ASL-MS TEMP	TEMP ERROR	NEW TEMP	TEMP ERROR	
103.80	209.30	208.90	208.70	2.20	209.60	-0.70	
110.71	209.90	209.40	207.30	2.10	210.20	-0.30	
117.94	210.50	209.90	207.90	2.00	210.90	-1.00	
125.50	211.10	210.40	208.90	1.90	211.60	-1.20	
133.40	211.70	210.90	209.20	1.70	212.20	-1.30	
141.65	212.30	211.50	210.00	1.50	212.90	-1.40	
150.26	212.90	212.00	210.80	1.20	213.60	-1.60	
159.23	212.80	211.90	210.90	1.00	213.50	-1.60	
168.58	212.70	211.80	211.20	0.60	213.50	-1.70	
178.32	212.70	211.80	211.50	0.30	213.50	-1.70	
188.45	212.60	211.70	211.80	-0.10	213.40	-1.70	
198.99	212.50	211.70	212.30	-0.60	213.40	-1.70	
209.94	212.40	213.60	214.70	-1.10	215.40	-1.80	
221.31	216.40	215.70	217.30	-1.60	217.50	-1.80	
233.12	218.40	217.80	220.00	-2.20	219.60	-1.80	
245.37	220.40	219.80	222.70	-2.90	221.60	-1.80	
258.08	222.70	222.20	225.70	-3.50	224.00	-1.80	
271.25	225.20	224.80	228.90	-4.10	226.60	-1.80	
284.89	227.60	227.20	231.90	-4.70	229.00	-1.80	
299.01	230.00	229.70	235.10	-5.40	231.60	-1.90	
313.63	232.60	232.30	238.10	-5.80	234.20	-1.90	
328.75	235.20	234.80	240.60	-6.00	236.70	-1.90	
344.38	237.80	237.40	243.60	-6.20	239.30	-1.90	
360.54	240.30	239.80	246.10	-6.30	241.80	-2.00	
377.23	242.80	242.20	248.40	-6.20	244.20	-2.00	
394.47	245.20	244.40	250.40	-6.00	246.50	-2.10	
412.26	247.70	246.70	252.50	-5.80	248.90	-2.20	
430.62	250.20	249.00	254.40	-5.40	251.20	-2.20	
449.56	252.60	251.20	256.00	-4.80	253.40	-2.20	
469.08	255.00	253.30	257.60	-4.30	255.60	-2.30	
489.20	257.40	255.40	259.10	-3.70	257.80	-2.40	
509.92	259.60	257.30	260.30	-2.00	259.70	-2.40	
531.28	261.60	259.00	261.30	-2.30	261.40	-2.40	
553.27	263.60	260.70	262.30	-1.60	263.20	-2.50	
575.89	265.60	262.30	263.30	-1.00	264.90	-2.60	
599.17	267.50	263.90	264.30	-0.40	266.50	-2.60	
623.11	269.50	265.60	265.40	0.20	268.20	-2.60	
647.72	271.40	267.20	266.50	0.70	269.90	-2.70	
673.03	273.30	268.80	267.70	1.10	271.50	-2.70	
699.03	275.10	270.30	268.90	1.40	273.00	-2.70	
725.74	276.60	271.60	269.90	1.70	274.30	-2.70	
753.17	278.00	272.80	270.90	1.90	275.50	-2.70	
781.34	279.40	273.90	271.80	2.10	276.70	-2.80	
810.25	280.80	275.00	272.80	2.20	277.80	-2.80	
839.91	282.10	276.10	273.90	2.30	278.90	-2.80	
870.35	281.60	275.50	273.10	2.40	278.30	-2.80	
901.56	282.50	275.20	272.60	2.00	277.80	-2.60	
933.57	283.40	275.20	272.60	2.60	277.80	-2.60	
966.38	284.30	275.20	272.60	2.60	277.80	-2.60	
1000.00	235.20	275.20	272.60	2.60	277.80	-2.60	
RMSASL 3.11	ABOVE,150 2.81		ABOVE,300 2.80		BELOW,300 3.72		TOTAL
RMSNEW 1.54	ABOVE,150 0.52		ABOVE,300 0.89		BELOW,300 2.46		TOTAL

CLCC TEMP P1 CLCC COVER CX1

269.000 0.090

57.68 44.19 41.24 55.45 70.90 83.52 110.40 86.26 103 6.80 33.46 1 PC1=APC2=0105.1

PRESSURE LEVEL	TRIAL TEMP	ACTUAL TEMP	ASL-MS TEMP	TEMP ERROR	NEW TEMP	TEMP ERROR
0.01	191.60	191.50	194.10	-2.60	191.60	-0.10
0.02	204.70	204.60	207.50	-2.50	204.70	-0.10
0.04	217.10	217.00	220.30	-3.30	217.20	-0.20
0.08	228.00	227.90	231.50	-3.60	228.10	-0.20
0.12	238.00	237.90	241.80	-3.90	238.10	-0.20
0.19	247.10	247.00	251.10	-4.10	247.20	-0.20
0.27	255.70	255.60	260.00	-4.40	255.80	-0.20
0.38	263.40	263.30	267.90	-4.60	263.50	-0.20
0.52	269.50	269.40	274.20	-4.80	269.60	-0.20
0.69	269.50	269.40	274.20	-4.80	269.60	-0.20
0.89	269.50	269.40	274.20	-4.80	269.60	-0.20
1.14	269.50	269.40	274.20	-4.80	269.60	-0.20
1.43	267.80	267.70	272.40	-4.70	267.90	-0.20
1.77	263.90	263.80	268.40	-4.60	264.00	-0.20
2.17	259.30	259.20	263.60	-4.30	259.40	-0.10
2.63	255.20	255.20	259.30	-4.10	255.30	-0.10
3.15	251.40	251.40	255.30	-3.90	251.60	-0.20
3.74	248.50	248.60	252.20	-3.60	248.70	-0.10
4.41	245.50	245.70	248.90	-3.20	245.80	-0.10
5.16	242.90	243.10	246.10	-3.00	243.20	-0.10
5.99	240.50	240.80	243.40	-2.60	240.90	-0.10
6.92	238.00	238.40	240.70	-2.30	238.50	-0.10
7.95	235.00	235.40	237.40	-2.00	235.50	-0.10
9.08	232.20	232.70	234.50	-1.80	232.70	0.0
10.32	223.10	223.60	225.10	-1.50	223.60	0.0
11.67	221.70	222.20	223.60	-1.40	222.30	-0.10
13.15	220.40	221.00	222.10	-1.10	221.00	0.0
14.76	219.10	219.70	220.70	-1.00	219.70	0.0
16.50	217.90	218.60	219.40	-0.80	218.50	0.10
18.39	216.70	217.40	218.00	-0.60	217.40	0.0
20.43	215.90	216.60	217.10	-0.50	216.60	0.0
22.62	216.20	217.00	217.30	-0.30	216.90	0.10
24.98	216.50	217.30	217.40	-0.10	217.30	0.0
27.50	216.70	217.60	217.50	0.10	217.50	0.10
30.21	216.90	217.90	217.50	0.40	217.70	0.20
33.09	215.70	216.70	216.20	0.50	216.60	0.10
36.17	214.50	215.50	214.80	0.70	215.40	0.10
39.45	213.30	214.40	213.40	1.00	214.20	0.20
42.94	212.20	213.30	212.20	1.10	213.10	0.20
46.64	211.00	212.10	210.80	1.30	212.00	0.10
50.56	210.00	211.20	209.70	1.50	211.00	0.20
54.72	209.50	210.70	209.00	1.70	210.50	0.20
59.11	209.10	210.30	208.50	1.80	210.10	0.20
63.75	208.60	209.90	207.80	2.10	209.60	0.30
68.64	208.10	209.40	207.20	2.20	209.20	0.20
73.80	208.10	209.40	207.00	2.40	209.20	0.20
79.22	208.30	209.60	207.10	2.50	209.40	0.20
84.93	208.50	209.80	207.10	2.70	209.60	0.20
90.92	208.70	210.00	207.20	2.80	209.80	0.20
97.21	208.80	210.10	207.20	2.90	210.00	0.10



SUMMARY RESULTS FOR DATE, SEP. 6, 76-LINE

SPECT 10 contd

TABLE II contd

CLCD TEMP PRESSURE LEVEL	PI TRIAL TEMP	CLOC COVER ACTUAL TEMP	CX1 ASL-MS TEMP	TEMP ERROR	NEW TEMP	TEMP ERROR	
103.80	209.30	210.00	207.70	2.30	210.50	0.10	
110.71	209.90	211.20	208.20	3.00	211.10	0.10	
117.94	210.50	211.70	208.80	2.90	211.70	0.0	
125.50	211.10	212.30	209.40	2.90	212.30	0.0	
133.40	211.70	212.80	210.10	2.70	212.90	-0.10	
141.65	212.30	213.30	210.80	2.50	213.60	-0.30	
150.26	212.90	213.80	211.50	2.30	214.20	-0.40	
159.23	212.80	213.00	211.70	1.90	214.10	-0.50	
168.58	212.70	213.40	211.80	1.60	214.00	-0.60	
178.32	212.70	213.20	212.10	1.10	214.00	-0.80	
188.45	212.60	213.00	212.40	0.60	213.90	-0.90	
193.99	212.50	212.70	212.80	-0.10	213.90	-1.20	
209.94	214.40	214.40	215.20	-0.80	215.80	-1.40	
221.31	216.40	216.20	217.80	-1.60	217.90	-1.70	
233.12	218.40	218.00	220.40	-2.40	219.90	-1.90	
245.37	220.40	219.80	223.00	-3.20	222.00	-2.20	
258.08	222.70	221.80	226.00	-4.20	224.30	-2.50	
271.25	225.20	224.10	229.10	-5.00	226.90	-2.80	
284.89	227.60	226.20	232.10	-5.90	229.40	-3.20	
299.01	230.00	228.40	235.20	-6.80	231.90	-3.50	
313.63	232.60	230.80	238.20	-7.40	234.50	-3.70	
328.75	235.20	233.70	240.90	-7.70	237.10	-3.90	
344.38	237.80	235.70	243.70	-8.00	239.70	-4.00	
360.54	240.30	238.10	246.20	-8.10	242.20	-4.10	
377.23	242.80	240.50	248.50	-8.00	244.70	-4.20	
394.47	245.20	242.80	250.60	-7.80	247.10	-4.30	
412.26	247.70	245.20	252.60	-7.40	249.20	-4.40	
430.62	250.20	247.70	254.60	-6.90	252.00	-4.30	
449.56	252.60	250.10	256.30	-6.20	254.30	-4.20	
469.08	255.00	252.40	258.00	-5.60	256.70	-4.30	
489.20	257.40	254.80	259.50	-4.70	259.00	-4.20	
509.93	259.60	257.00	260.70	-3.70	261.00	-4.00	
531.28	261.60	259.00	261.80	-2.80	262.90	-3.90	
553.27	263.60	261.00	262.90	-1.90	264.80	-3.80	
575.89	265.60	263.00	264.00	-1.00	266.60	-3.60	
599.17	267.50	264.90	265.00	-0.10	268.40	-3.50	
623.11	269.50	266.90	266.20	0.70	270.20	-3.30	
647.72	271.40	268.70	267.40	1.30	271.90	-3.20	
673.03	273.30	270.60	268.60	2.00	273.70	-3.10	
699.03	275.10	272.40	269.80	2.60	275.30	-2.90	
725.74	276.60	273.80	270.80	3.00	276.60	-2.80	
753.17	278.00	275.20	271.80	3.40	277.90	-2.70	
781.34	279.40	276.50	272.80	3.70	279.00	-2.50	
810.25	280.80	277.90	273.80	4.10	280.20	-2.30	
839.91	282.10	279.10	274.80	4.30	281.30	-2.20	
870.35	281.60	278.60	274.20	4.40	280.70	-2.10	
901.56	282.50	278.80	273.70	5.10	280.10	-1.30	
933.57	283.40	278.80	273.70	5.10	280.10	-1.30	
966.38	284.30	278.80	273.70	5.10	280.10	-1.30	
1000.00	285.20	278.80	273.70	5.10	280.10	-1.30	
RMSASL 3.76	ABOVE, 150 2.86		ABOVE, 300 2.97		BELOW, 300 5.15		TOTAL
RMSNEW 1.99	ABOVE, 150 0.16		ABOVE, 300 0.89		BELOW, 300 3.38		TOTAL

#### 1.4 COMPOSITION PROFILE STUDIES

#### 1.4.1 SUMMARY

NOAA-2 satellite radiance measurements and correlated radiosonde temperature and dew-point temperature profiles for the WSMR Region were used to determine the variability of atmospheric  $\text{CO}_2$ , for different altitudes, by asymptotic solution of the Ladenberg-Reiche equation. Thirty-four sets of data were available for use. Transmittances used in the retrieval were corrected using the measured temperature and dew-point temperature profiles. Preliminary results indicate a lowered daylight period atmospheric  $\text{CO}_2$  mixing ratio at high altitude (as compared to the accepted standard mixing ratio). This appears to be consistent with a previous result indicating a diurnal  $\text{CO}_2$  mixing ratio variation (Bruce et. al. 1975).

An iteration technique, due to Chahine (1972), was attempted on the data with very unsatisfactory results. Through the use of synthetic studies, the problems in determining  $\text{CO}_2$  composition appear to be the result of cloud contamination, inadequacy in the transmittance model and the temperature dependence of the weighing function.

The study indicates that the technique should be usable for  $\text{H}_2\text{O}$  determination using VTPR channels 7 and 8 (and possibly channel 6) if the cloud problem can be satisfactorily solved.



#### 1.4.2 PERTURBATION TECHNIQUE RESULTS

##### Basic Formulation

The method used to solve the radiative transfer equation (RET) by perturbation technique for the CO<sub>2</sub> composition profile,  $q$ , is basically that proposed by M. T. Chahine (1972). The outgoing radiance at frequency  $\nu$ , from a non-scattering atmosphere in local thermodynamic equilibrium, observed from pressure  $\bar{p}$  can be expressed as

$$I_{\nu}(\bar{p}) = B_{\nu}[T(\bar{p})] - \int_{\ln p_0}^{\ln \bar{p}} \tau_{\nu}[q_i(p), T(p)] \frac{\partial B_{\nu}[T(p)]}{\partial \ln p} d \ln p, \quad (1)$$

in which  $B(T)$  is the Planck function,  $p_0$  is ground surface pressure and  $\tau$  is the transmittance from pressure level  $p$  to  $\bar{p}$ . It is noted that the transmittance  $\tau$  is a function principally of the composition profiles,  $q_i(p)$ , of the several absorbing species as well as of temperature,  $T$ . There is one such equation for each radiometer channel. The usual practice is to express the total transmittance as the product of separable CO<sub>2</sub>, H<sub>2</sub>O and O<sub>3</sub> transmittances,

$$\tau(q_1, q_2, q_3, T) = \prod_{i=1}^3 \tau_i(q_i, T). \quad (2)$$

In this analysis, rather than solving for the CO<sub>2</sub> composition profile  $q_i(p)$  we solve for the relative CO<sub>2</sub> profile,  $\alpha(p)$ , defined by

$$q(p) = \alpha(p) q_{\text{std}}(p), \quad (3)$$

where  $q_{\text{std}}(p)$  is the CO<sub>2</sub> composition profile used in the standard transmittances.

In order to solve (1) for the parameter  $\alpha(p)$ , we note that the major contribution to the outgoing radiance comes from the atmospheric region centered about the peak of the weighting function; that is, the pressure  $p_m$  for which  $\partial\tau/\partial \ln p$  reaches its maximum value. For a particular frequency  $\nu$ , solution of (1) yields a value of  $\alpha_\nu(p_m)$  representative of the relative composition profile at pressure  $p_m$ . Since the optical depth in this region is on the order of 1 or greater, strong line absorption is valid (Kaplan, 1953). The parameter  $\alpha_\nu$  can be related to  $\tau$  standard through asymptotic solution of the Ladenberg-Reiche equation (Chahine, 1972),

$$\tau_{\text{co}_2}(\alpha_\nu q_{\text{std}}, T) \approx \tau_{\text{co}_2}(q_{\text{std}}, T) \sqrt{\alpha_\nu}. \quad (4)$$

In accordance with Chahine (1972) a direct first order perturbation solution for  $\alpha_\nu$  leads to

$$\alpha_\nu = \left\{ 1 - (I_\nu - I_\nu) \int_{\ln p_0}^{\ln \bar{p}} \tau_{\text{total}} \ln \tau_{\text{co}_2} \frac{\partial B(T)}{\partial \ln p} d \ln p \right\}^{1/2}, \quad (5)$$

in which  $\tau_{\text{total}}$  is defined by (2). The relative  $\text{CO}_2$  composition in the region of the weighting function centroid for each radiometer channel is obtained from (5) if one knows the temperature corrected standard  $\text{CO}_2$  transmittances,  $\text{H}_2\text{O}$  and  $\text{O}_3$  transmittances and the temperature profile. This approximate solution for  $\alpha$  becomes questionable when it deviates substantially from the value of 1, since the first neglected term in the expansion of  $\tau^{\sqrt{\alpha}}$  becomes non-negligible for  $\alpha < 0.4$  or  $\alpha > 1.6$ . Further, for  $\alpha < 0.6$  one questions the Ladenberg-Reiche asymptotic solution.

## Data

Thirty-four sets of data correlating temperature and dew-point radiosonde measurements over WSMR, with NOAA-2 VTPR soundings were available for this study. All VTPR soundings over WSMR, or immediately adjacent to the range, are being processed for a  $\text{CO}_2$  perturbation determination. As of the close of the contract year all of the available data had not been processed. A reasonable amount of time is required to select the specific VTPR soundings to be processed from the 49 blocks in each set. Each sounding location must be plotted on a map of the WSMR region.

## Results

Figure IV-1 through IV-7 illustrates the typical results obtained using this technique. Figure IV-1 and IV-2 show the radiosonde water vapor and temperature profiles for the particular sounding set. The next five figures show the inferred  $\text{CO}_2$  mixing ratios for each of the five VTPR soundings on or adjacent to WSMR. The vertical axis for each plot is the standard VTPR transmittance-pressure level, numbering 1 at the top of the atmosphere and 100 at the bottom. (The number "101" is an artifact of the plotter.) Each of the  $\text{CO}_2$  profile plots show  $\text{CO}_2$  for the measured temperature and watervapor.. circles; and the probable limits of accuracy assuming 10% watervapor fluctuation and  $\pm 1^\circ\text{K}$ . in the temperature measurement.

## Discussion

Comparison of the results with the temperature profile indicates that the  $\text{CO}_2$  determination for pressure level 55 (VTPR channel 3) is invalid--the temperature is essentially isothermal in this region. The determination for pressure level 45 (VTPR channel 2) is very suspect for similar reasons.

The large variation of  $\text{CO}_2$  near ground level is difficult to explain with the limited data processed to date. It may represent actual fact; however, it more probably is the result of either cloud contamination, ground level altitude variations, ground emissivity variations or extreme water vapor variations over the region--or a combination of these.

We believe that the  $\text{CO}_2$  mixing ratios for channels 1 and 4 are the most dependable values.

It is the intent of the authors to make a thorough error analysis of all results of this study and combine the results of this study with those of the previous SIRS study (Bruce et. al., 1975). A technical report and possibly an open literature report of the combined studies will be prepared, hopefully by February 1977.



### 1.4.3 ITERATION TECHNIQUE RESULTS

#### Basic Formulation

As originally formulated by Smith (1970) and extended by Chahine (1972) equation 1 may be solved for the scaling constant  $\alpha$ , equation 3, using an iterative technique. Since a separate  $\alpha_j$  is determined for each VTPR channel, the technique requires convergence on an atmospheric profile  $\bar{\alpha}_i$  defined by

$$\bar{\alpha}_i = \frac{\sum_{j=1}^J \alpha_j W(\nu_j, p_i)}{\sum_{j=1}^J W(\nu_j, p_i)} \quad (6)$$

where

$\alpha_j$  = scaling constant for the  $j^{\text{th}}$  VTPR channel

$p_i$  =  $i^{\text{th}}$  VTPR pressure level

$W(\nu_j, p_i)$  = weighting function for the  $j^{\text{th}}$  VTPR channel at pressure level  $p_i$ .

Determination of the weighting function requires a model for the  $\text{CO}_2$  transmittance: the  $n^{\text{th}}$  iteration weighting function is given by

$$W^{(n)}(\nu_j, p_i) = \left[ \frac{\partial \tau(\nu_j, p_i)}{\partial \alpha} \right]^{(n-1)} \cdot \frac{\partial B(\nu_j, p_i)}{\partial \ln p}, \quad (7)$$

in which  $B(\nu_j, p_i)$  is the Planck function for the  $j^{\text{th}}$  VTPR channel frequency at pressure level  $p_i$ . It is through Planck term that the temperature profile enters the problem. It is obvious that for an isothermal temperature region, no composition information can be obtained.

For the iteration technique the NOAA-2 zenith angle correction model was utilized. This model is inadequate since only the linear terms in  $\alpha$

of a Smith Polynomial model are Used:

$$\mathcal{Z}_j(\alpha_j, T_i, P_i) = \mathcal{Z}_j(q_j, T_i, P_i) \exp[B_j \ln(\alpha)] \quad (8)$$

in which for the  $j^{\text{th}}$  channel,

$$(B_j)_i = 0.1 \left[ C_{1j} + C_{2j} PE_i + C_{3j} TE_i + C_{4j} TE_i PE_i + C_{5j} TE_i^2 \right] \quad (9)$$

where for pressure level  $P_i$ ,

$$TE_i = \ln(TX_i / 273) \quad ,$$

$$PE_i = \ln(P_i / 2000) \quad ,$$

and

$$TX_i = \frac{1}{P_i} \int_{P_0}^{P_i} T(P) dP \quad .$$

Using this model the first term in the weighting function for the  $j^{\text{th}}$  VTPR channel and pressure level  $P_i$  is given by

$$\frac{\partial \mathcal{Z}_j(P_i)}{\partial (\alpha_j)_i} = \mathcal{Z}_j(P_i) \ln[\mathcal{Z}_j(P_i)] (B_j)_i \Delta P_i / (P_i \bar{\alpha}_i) \quad (10)$$

for which

$$\bar{\alpha}_i = \left[ \sum_{k=1}^L \bar{\alpha}_k (P_k - P_{k-1}) \right] / P_i \quad (11)$$

An iterative computer scheme based upon the Chahine technique, which is similar in nature to the temperature retrieval iterative schemes, was written for the University IBM computer.

#### Computer Results and Difficulties

Excessive convergence difficulties were encountered when the WSMR data was utilized. The primary suspected cause for this problem (outside of programming error) was the transmittance model. To test the adequacy of the program and the transmittance model, synthetic data was prepared: transmittances for various  $\text{CO}_2$  profiles were computed using the model and in turn used to compute synthetic radiances for the observed temperature and watervapor for one particular set of data. These synthetic radiances, the temperature profile and watervapor profile were used as input for the iteration program. While convergence was slow, it was obtained; and the resulting computed  $\text{CO}_2$  profiles for all but one case were within tolerable limits of the correct value. Computer output for the convergent cases are shown in Figures IV-8 through IV-17. The assumed temperature profiles and watervapor profiles used for the calculation are shown in Figures IV-8 and IV-9. The remaining figures in the set are ordered so that the  $\text{CO}_2$  profile used in the radiance calculation is followed by the retrieved  $\text{CO}_2$  profile.

Figure IV-18 shows the final weighting functions for case 4. Comparison of the retrieved profile with the actual profile for case 4 (figures IV-17 and IV-16) shows a discrepancy at both the top and the bottom of the atmosphere. This is explained by the fact that the weighting functions fall off to zero at their pressure levels. Figure IV-18 also indicates the

effect of the isothermal region of the temperature profile: little or no information can be obtained about the region near the tropopause. We believe that this effect may be the cause of the non-convergence in case 5 (Figures IV-19 and IV-20): too little  $\text{CO}_2$  is determined in the tropopause region and too much in the lower atmosphere. This case also probably indicates a difficulty with the model; second order terms in  $\alpha$  are needed.

#### Discussion

The synthetic study indicates that the computer algorithms are programmed correctly. We feel that the lack of convergence using actual data can be traced to either a) inadequate transmittance model or b) cloud contamination, or a combination of the two. The former of the two is clearly indicated by examination of figure IV-18: essentially only two regions of the atmosphere can be sensed for  $\text{CO}_2$  using the inadequate transmittance model.

At present we are working on obtaining a better  $\text{CO}_2$  model. With this anticipated improvement and assuming that the clear channel radiances can be determined, we believe that it is possible to obtain good  $\text{CO}_2$  profiles. Even without cloud corrections, it appears that upper channel  $\text{CO}_2$  values can be obtained.



#### 1.4.4 RECOMMENDATIONS FOR FURTHER WORK

So that this effort can be brought to a successful conclusion, we recommend that the following be undertaken.

a) A more adequate  $\text{CO}_2$  transmittance model for NOAA-2 transmittances should be constructed. We believe that a Smith type polynomial containing at least second order terms in composition (and preferably third order) is needed. Work on this will continue.

b) Cloud correction techniques should be applied to the radiances used for the  $\text{CO}_2$  retrievals. At this time it is not clear which of the several cloud correction techniques reported elsewhere herein will be the most effective.

c) The iteration technique should be utilized to determine  $\text{H}_2\text{O}$  content in the temperature retrieval program. A preliminary effort is underway to demonstrate that channels 7 and 8 or channels 6, 7 and 8 can be used for this purpose. Of great interest will be the effect of water normalization using a trial temperature on the retrieved temperature profile.

d) Cloud correction techniques should be incorporated into the  $\text{H}_2\text{O}$  retrieval subroutine.

#### 1.4.5 BIBLIOGRAPHY

Bruce, R. E., C. Manquero and L. D. Duncan, 1975: "Atmospheric CO<sub>2</sub> Variability Determined from Satellite Measurements", ECOM Report.

Chahine, M. T., 1972: "A General Relaxation Method for Inverse Solution of the Full Radiative Transfer Equation", J. Atmos. Sci., 29, 741-747.

Kaplan, L. D., 1959: "Inference of Atmospheric Structure from Remote Radiation Measurements", J. Opt. Soc. Amer., 49, 1004-1007.

Smith, W. L., 1970: "Iterative Solution of the Radiative Transfer Equation for the Temperature and Absorbing Gas Profile of an Atmosphere", Appl. Opt., 9, 1993-1999.

#### 1.4.6 FIGURES

# WATER VAPOR PROFILE 20FEB75

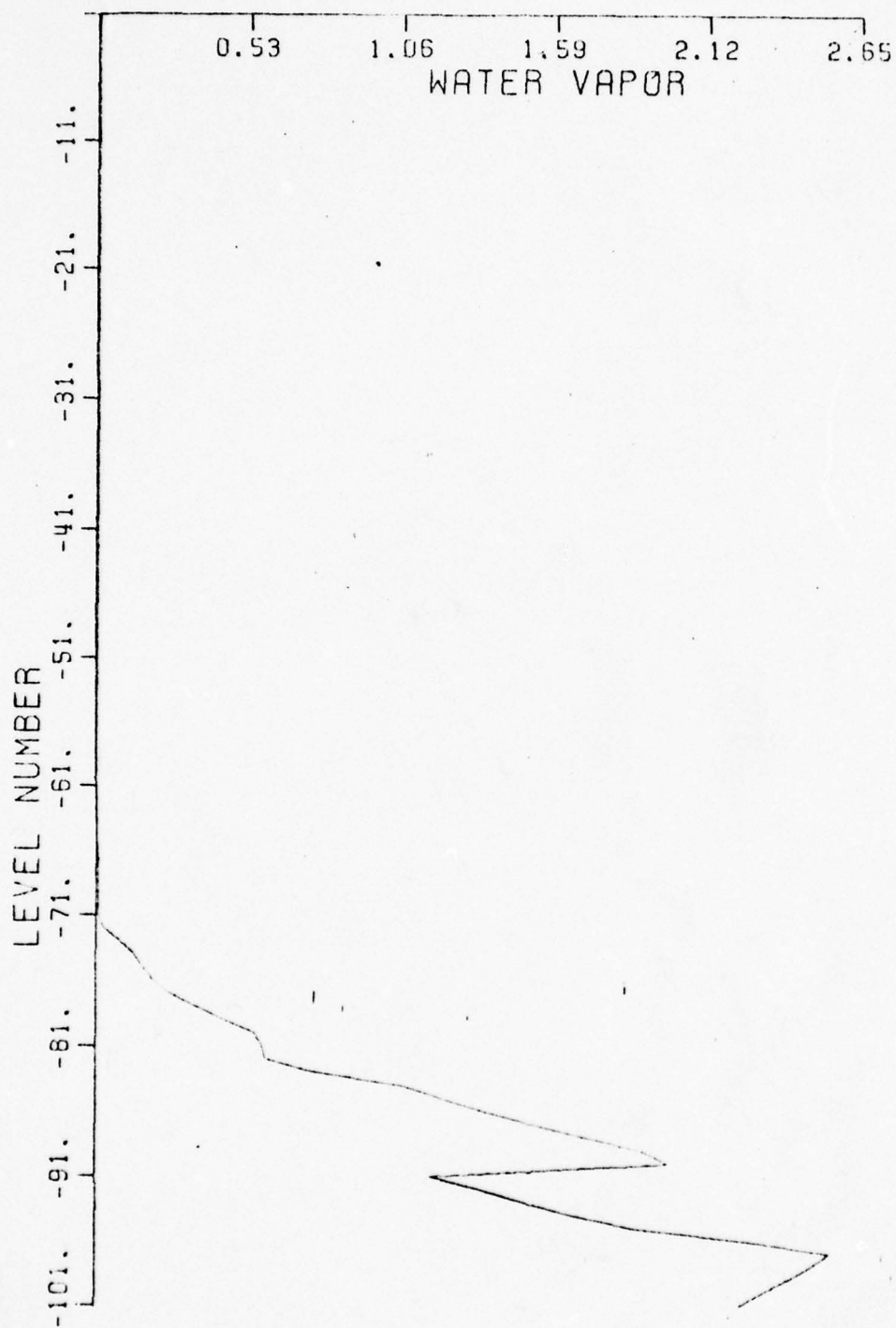


Figure IV-1



# TEMPERATURE PROFILE 20FEB75

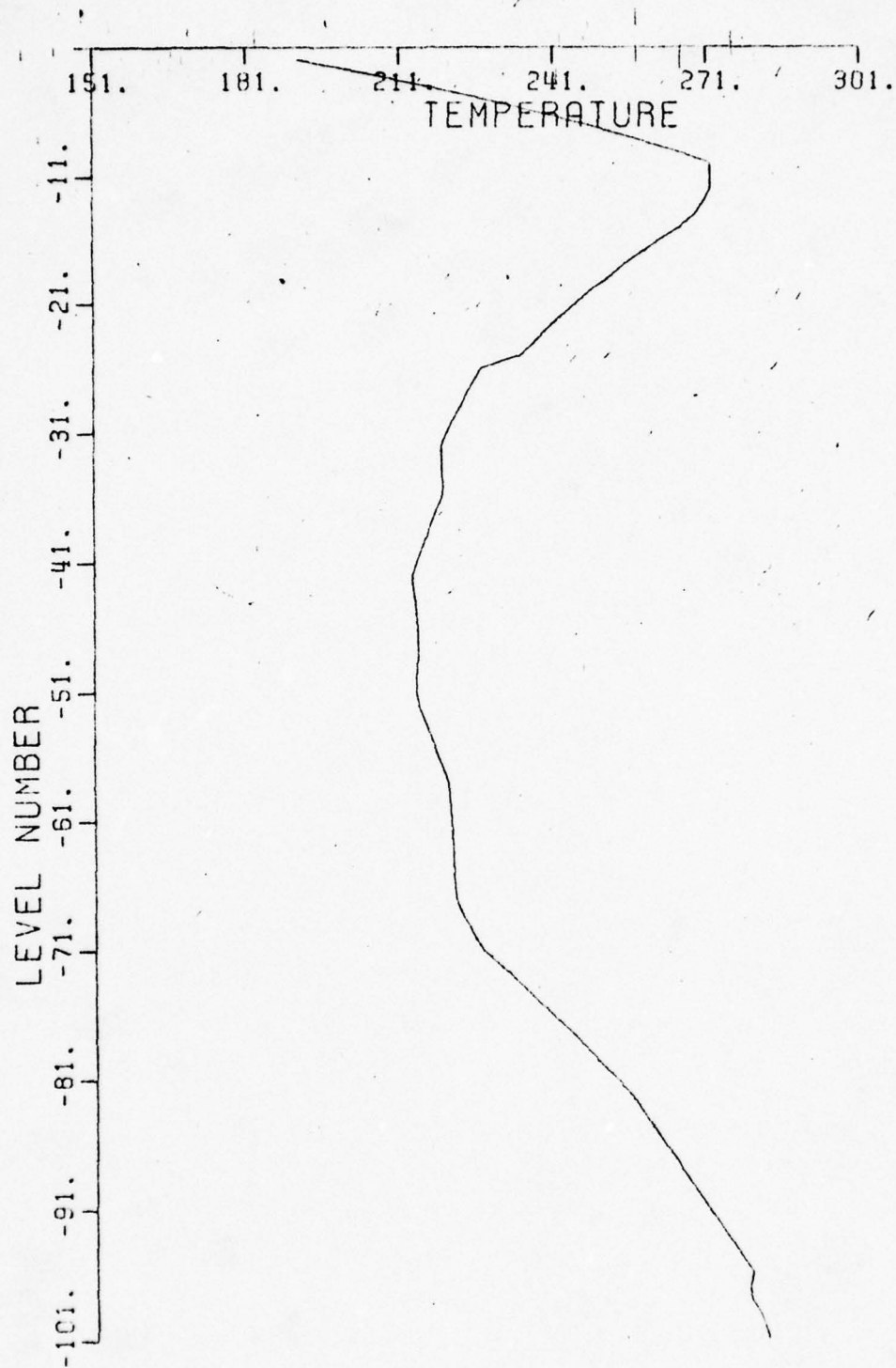


Figure IV-2

CO2 PROFILE 20FEB75 17 6,  
 CIRCLE=T, TRIANGLE=T-1, PLUS=T+1  
 ZENITH ANGLE= 17.00 DEGREES

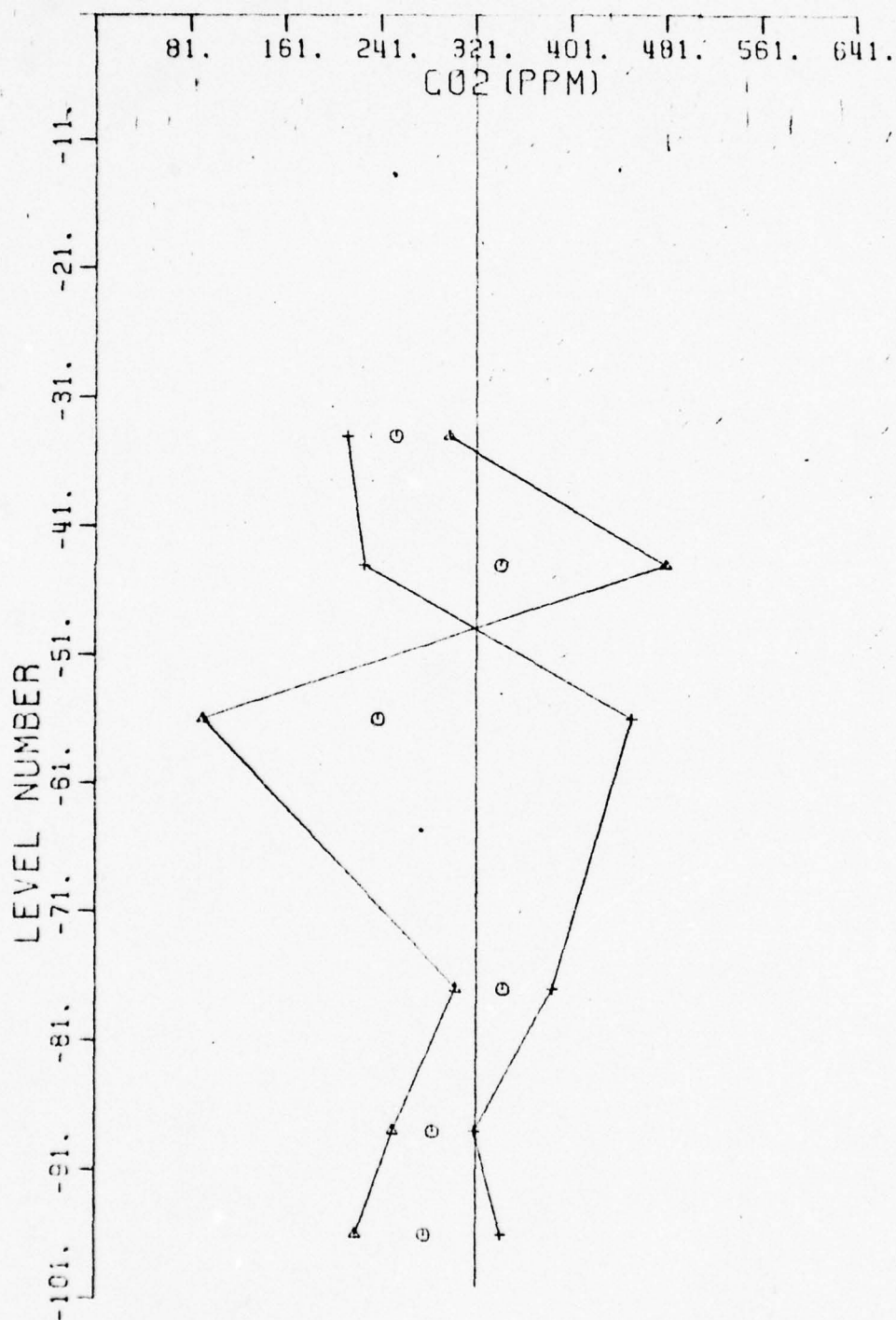


Figure IV-3

CO2 PROFILE 20FEB75 18 6  
 CIRCLE=T, TRIANGLE=T-1, PLUS=T+1  
 ZENITH ANGLE= 20.50 DEGREES

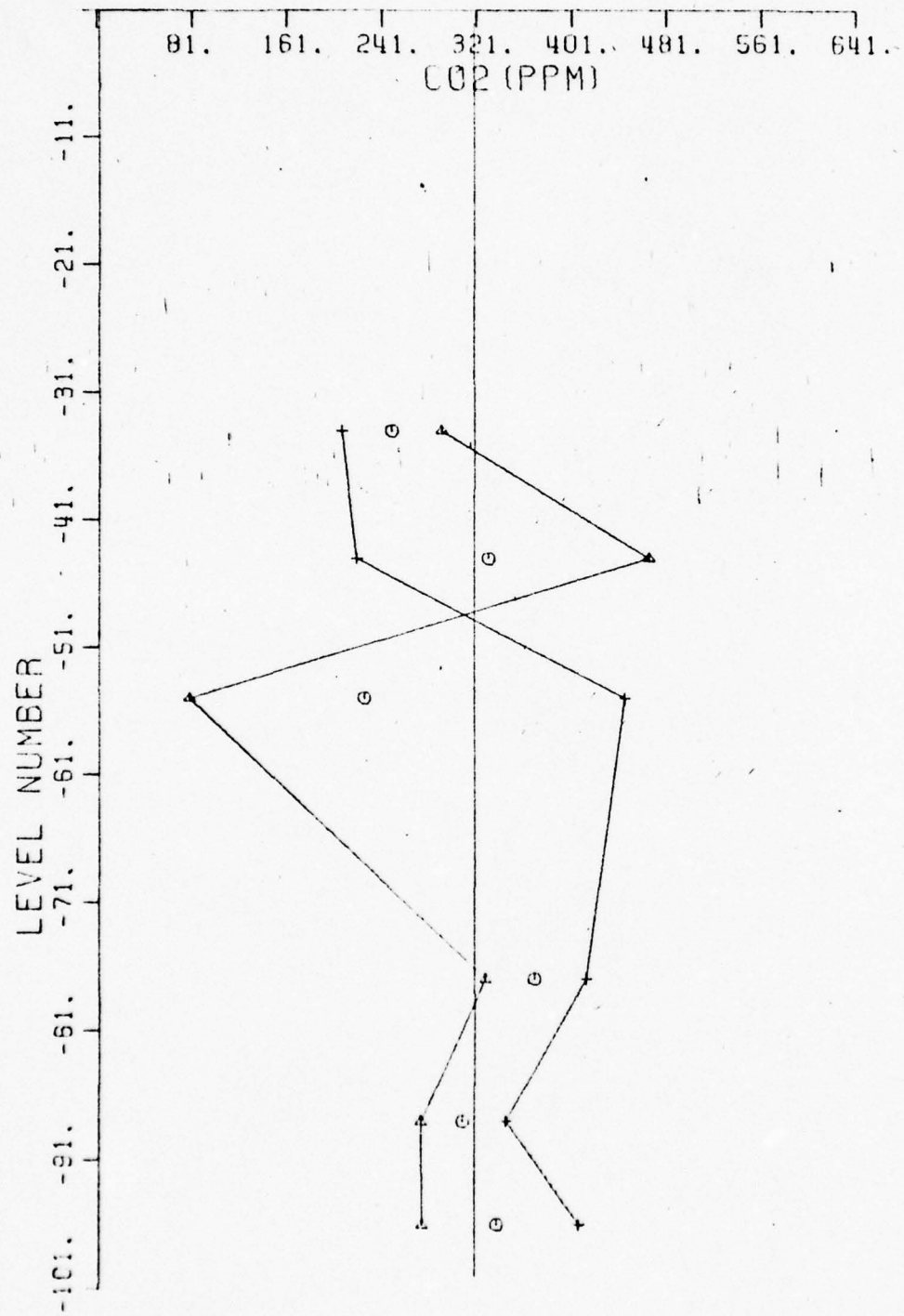


Figure IV-4

CO2 PROFILE 20FEB75 16 7  
 CIRCLE=T, TRIANGLE=T-1, PLUS=T+1  
 ZENITH ANGLE= 13.60 DEGREES

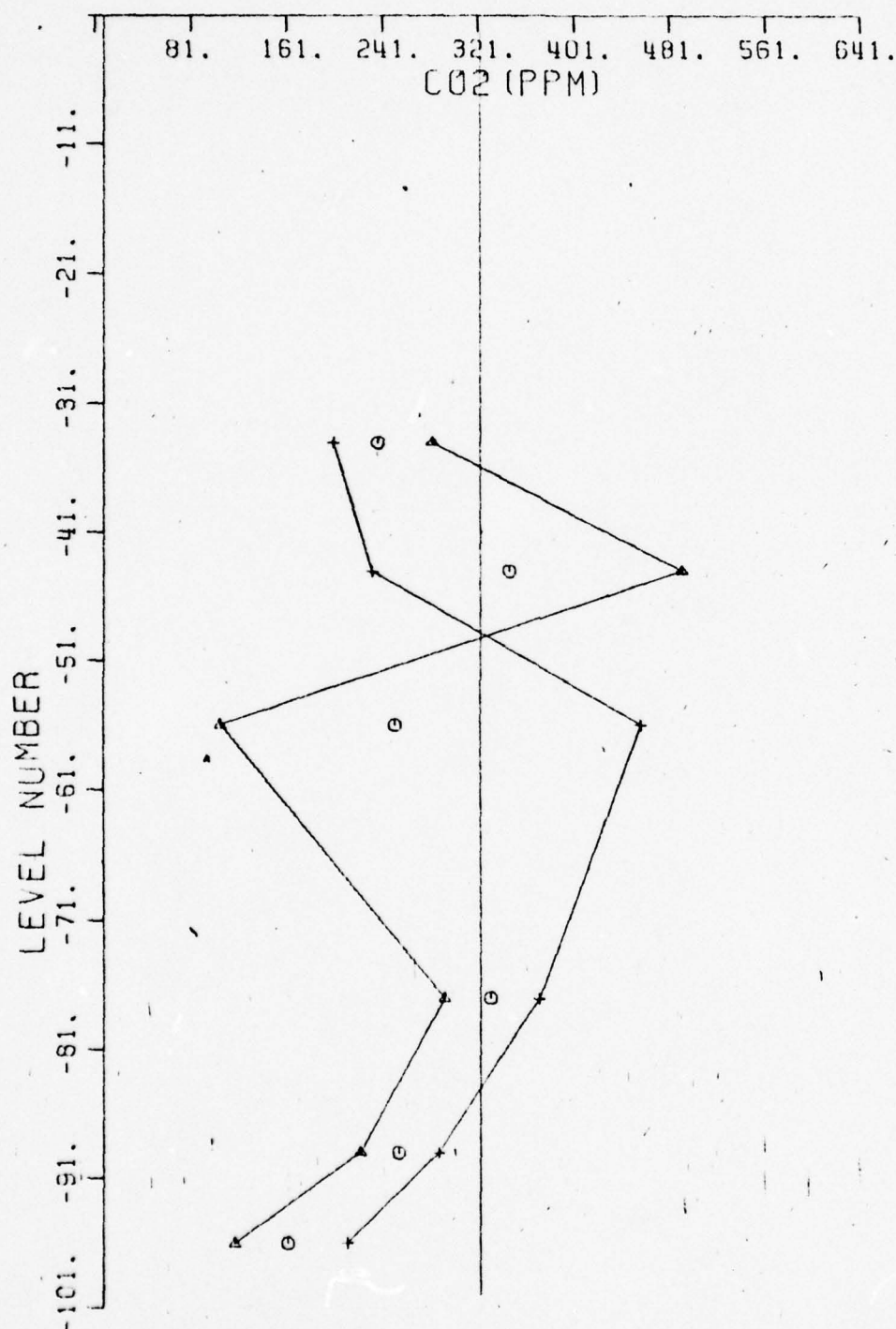


Figure IV-5



CO2 PROFILE 20FEB75 17 7  
 CIRCLE=T, TRIANGLE=T-1, PLUS=T+1  
 ZENITH ANGLE= 17.00 DEGREES

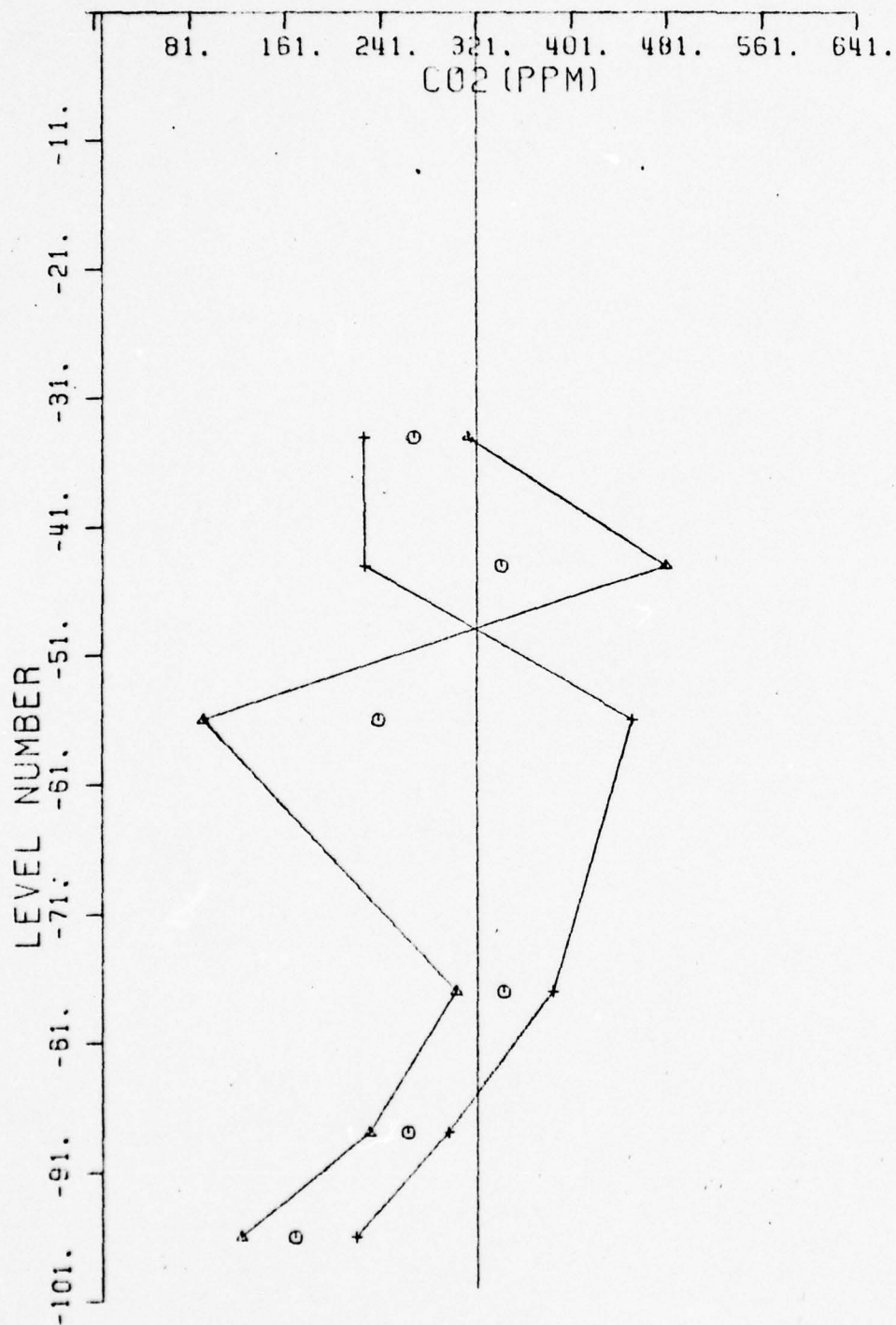


Figure IV-6

CO2 PROFILE 20FEB75 AVERAGED RADIANCES  
 CIRCLE=T, TRIANGLE=T-1, PLUS=T+1  
 AVERAGE ZENITH ANGLE= 17.02 DEGREES

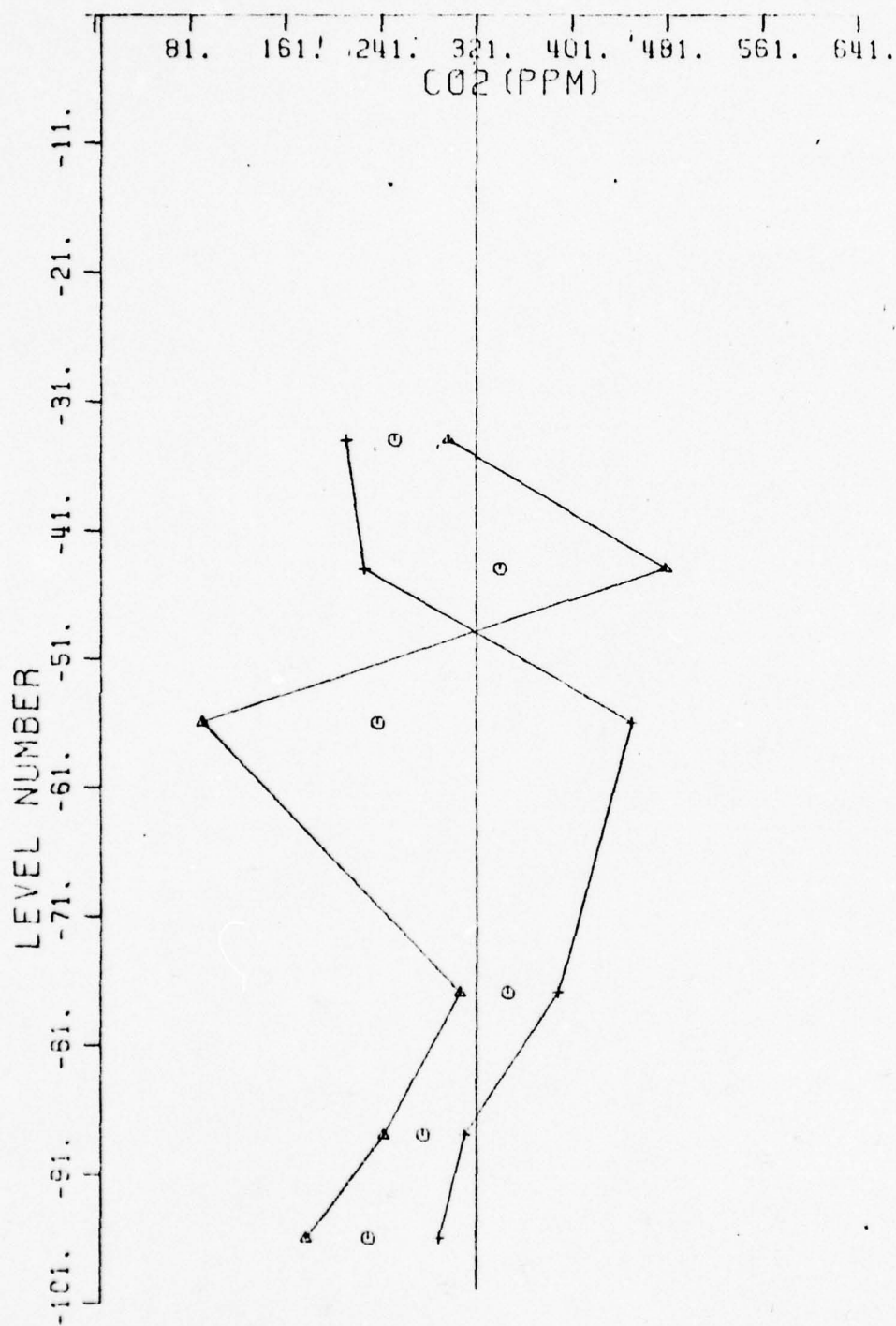


Figure IV-7

# TEMPERATURE PROFILE 2/27/75

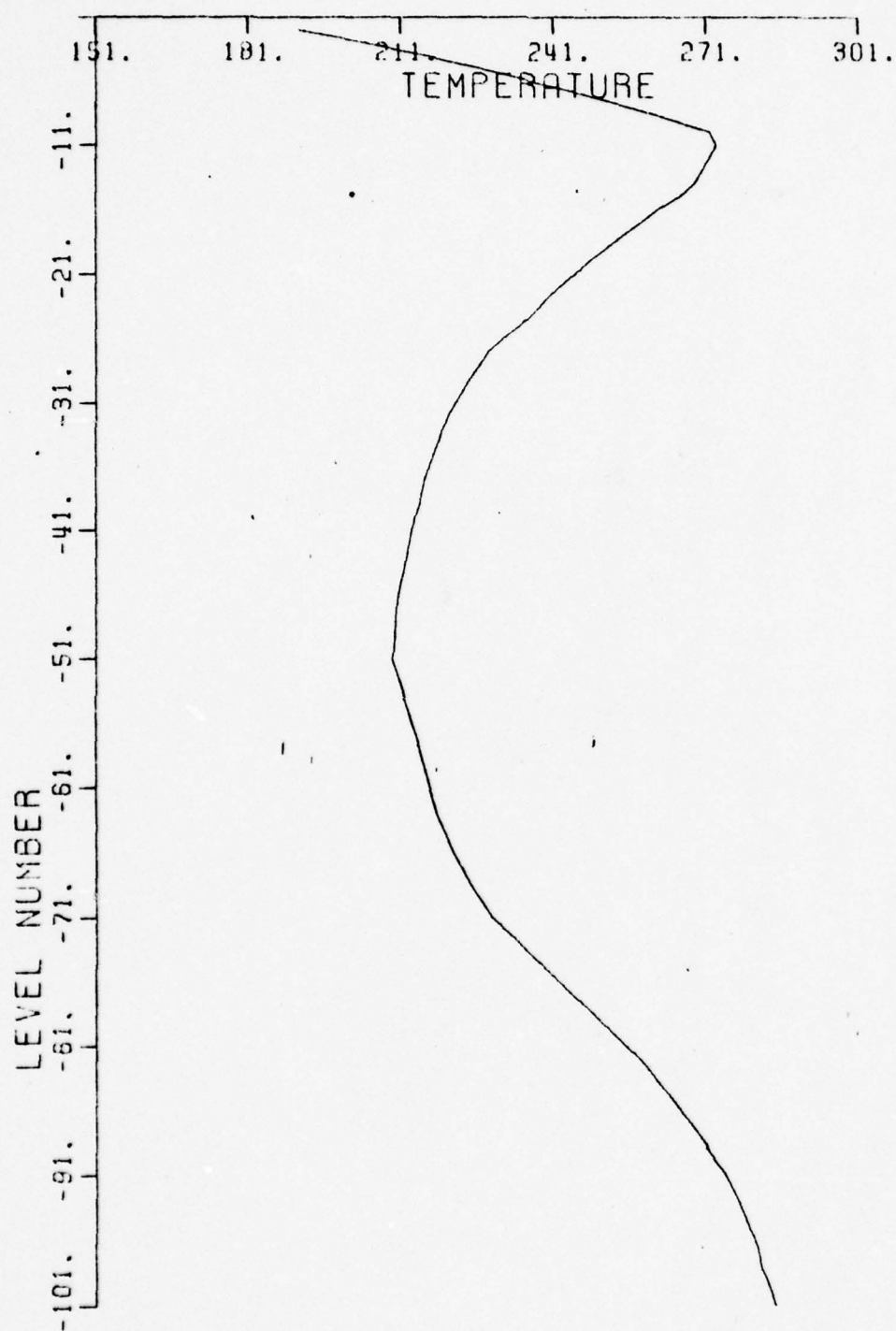


Figure IV-8. Temperature profile used for synthetic study.

# WATER VAPOR PROFILE 2/27/75

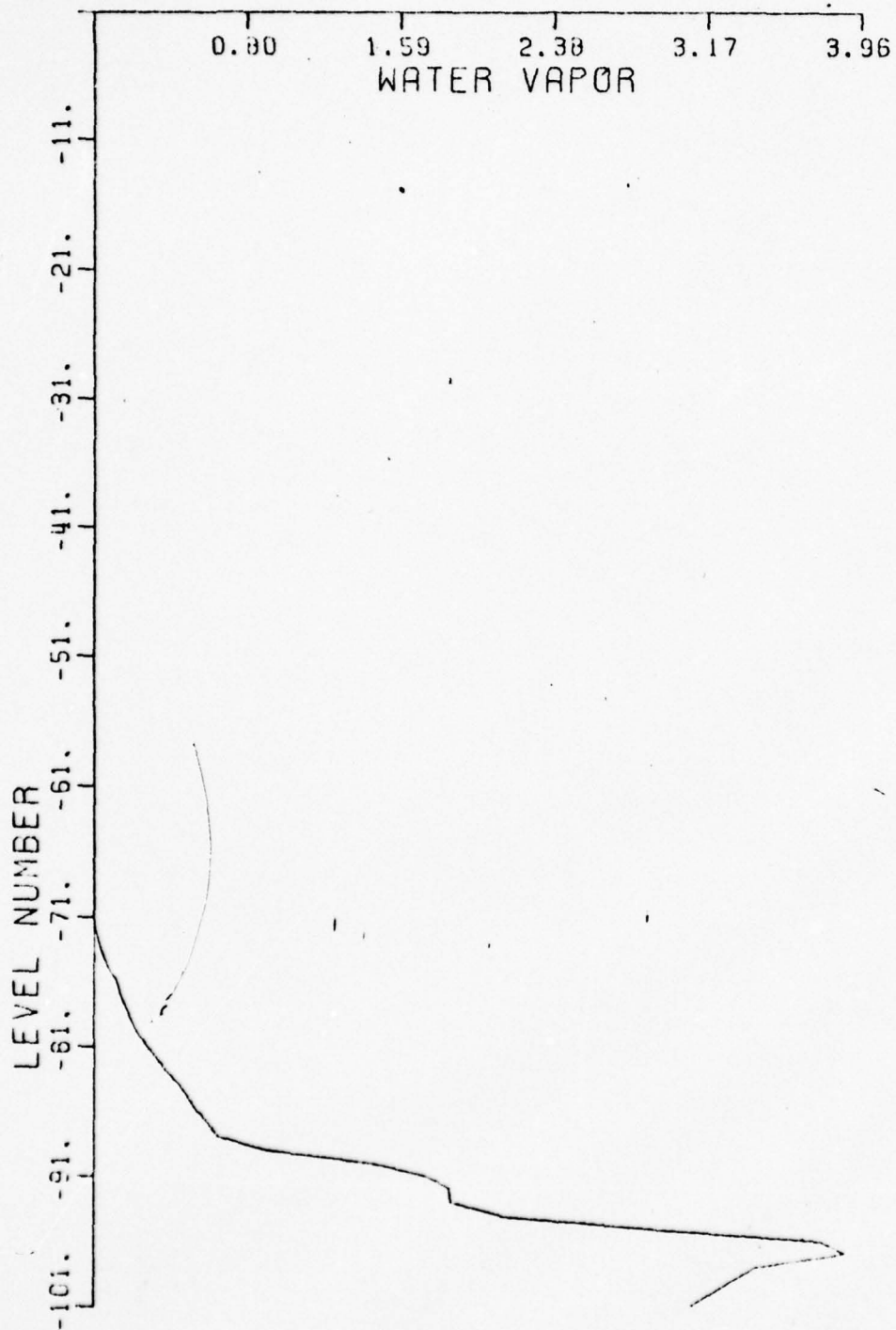


Figure IV-9. Water vapor profile use for synthetic study.



CO2 PROFILE 2/27/75 53  
CIRCLE=T0, TRIANGLE=T0-1, PLUS=T0+1

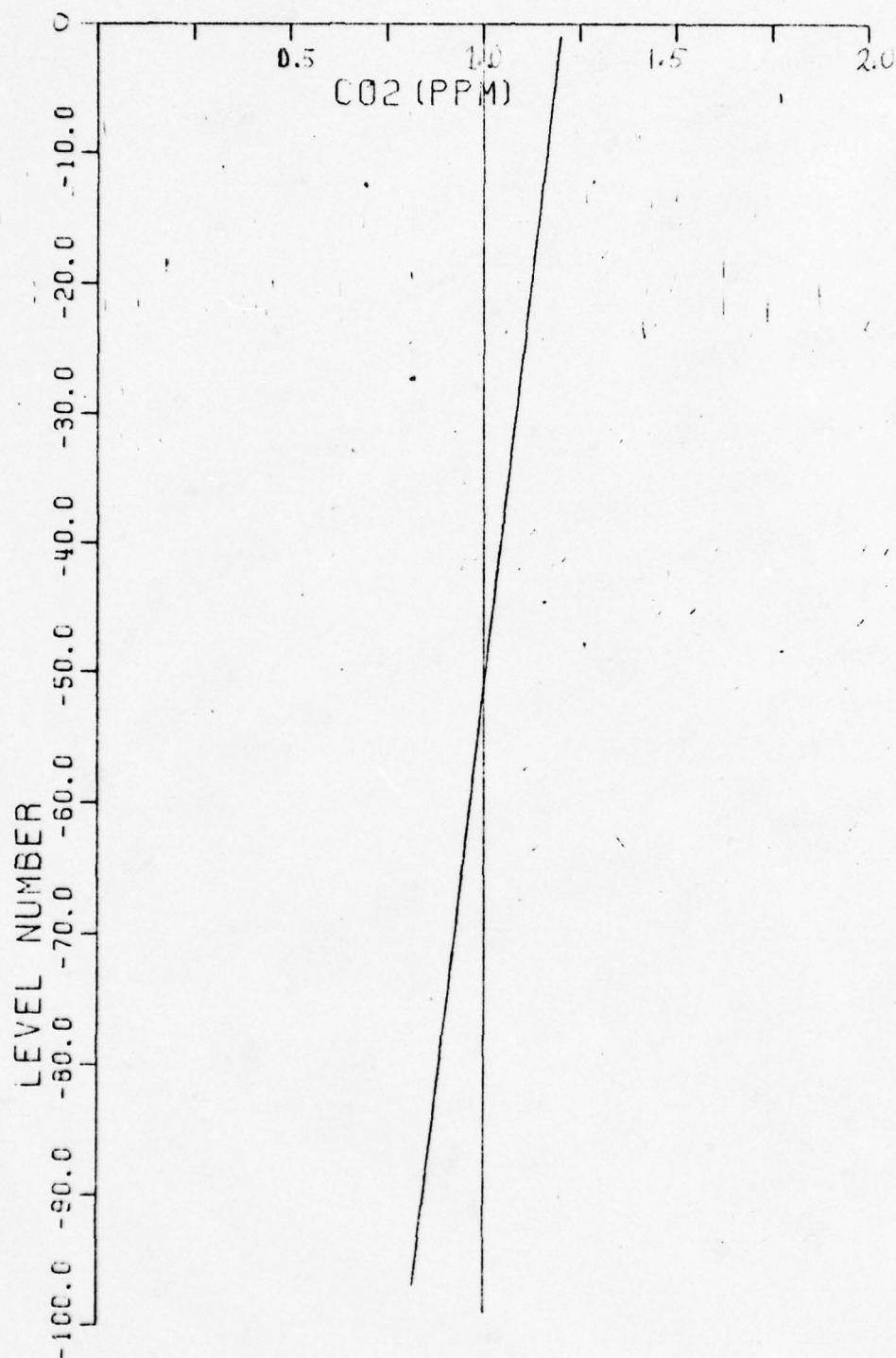


Figure IV-10. Case 1 actual CO<sub>2</sub> profile used to calculate radiances.

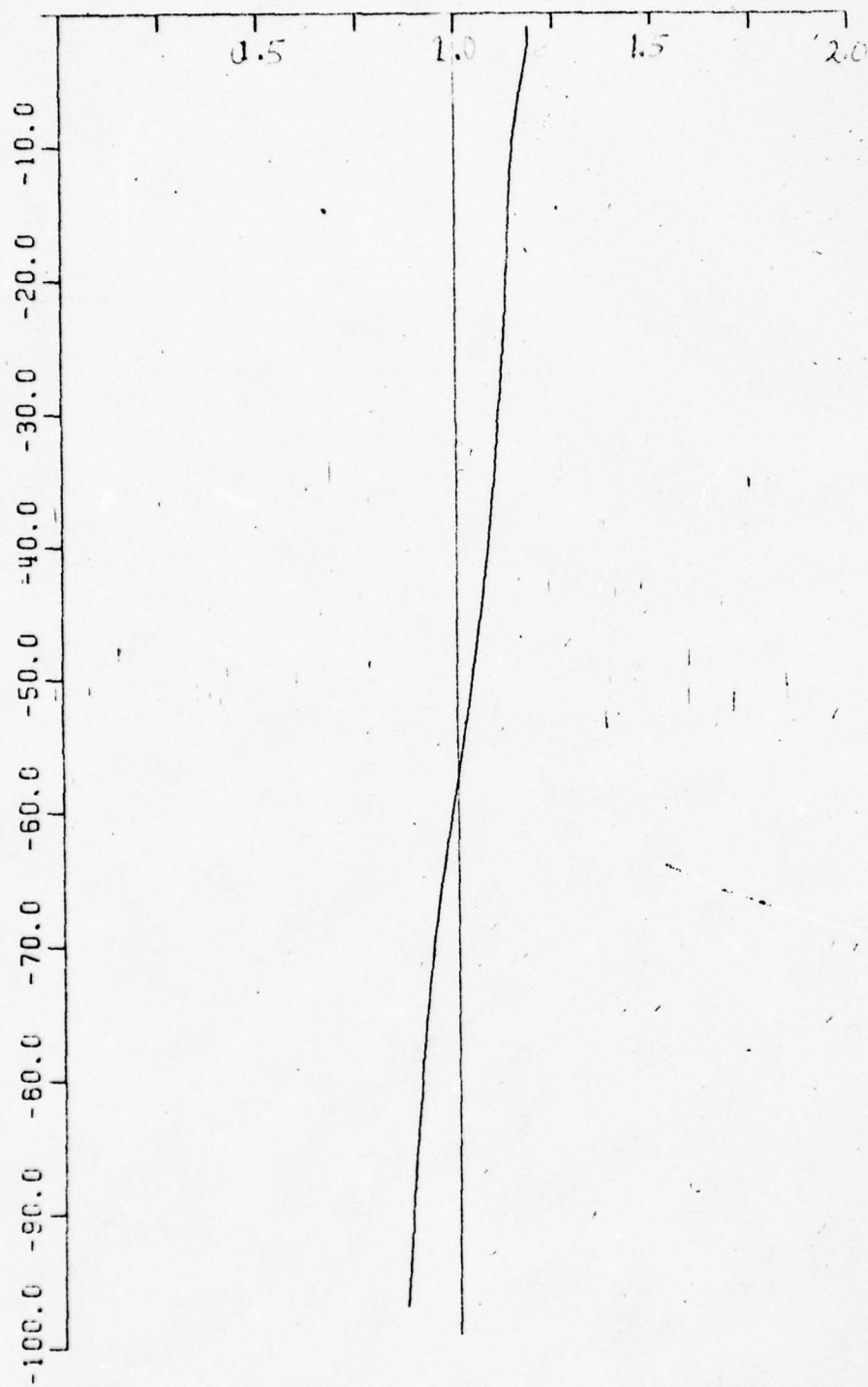


Figure IV-11. Retrieved CO<sub>2</sub> profile Case 1.

CO2 PROFILE 2/27/75 53  
CIRCLE=T0, TRIANGLE=T0-1, PLUS=T0+1

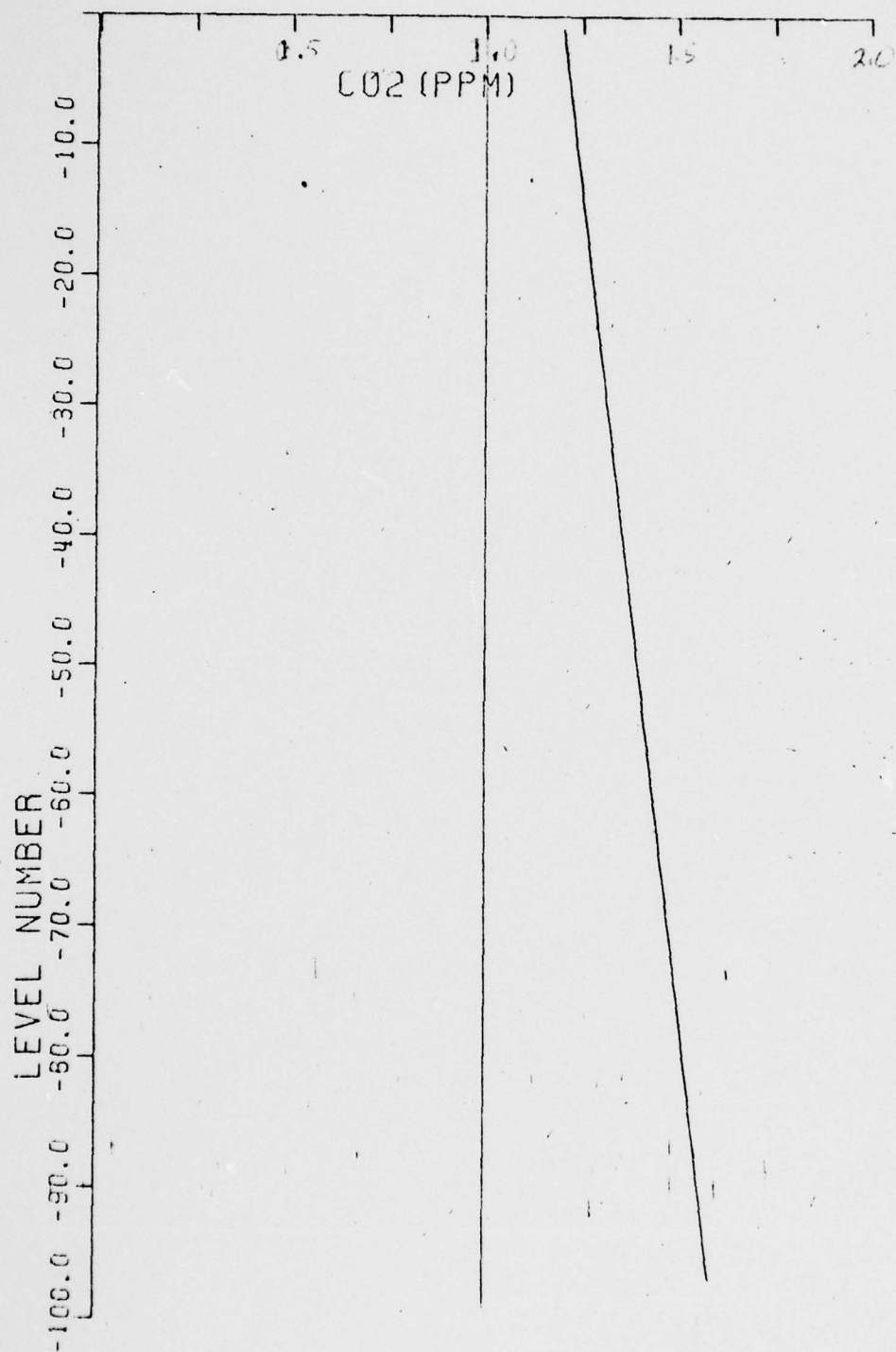


Figure IV-12. Actual CO<sub>2</sub> profile for Case 2.

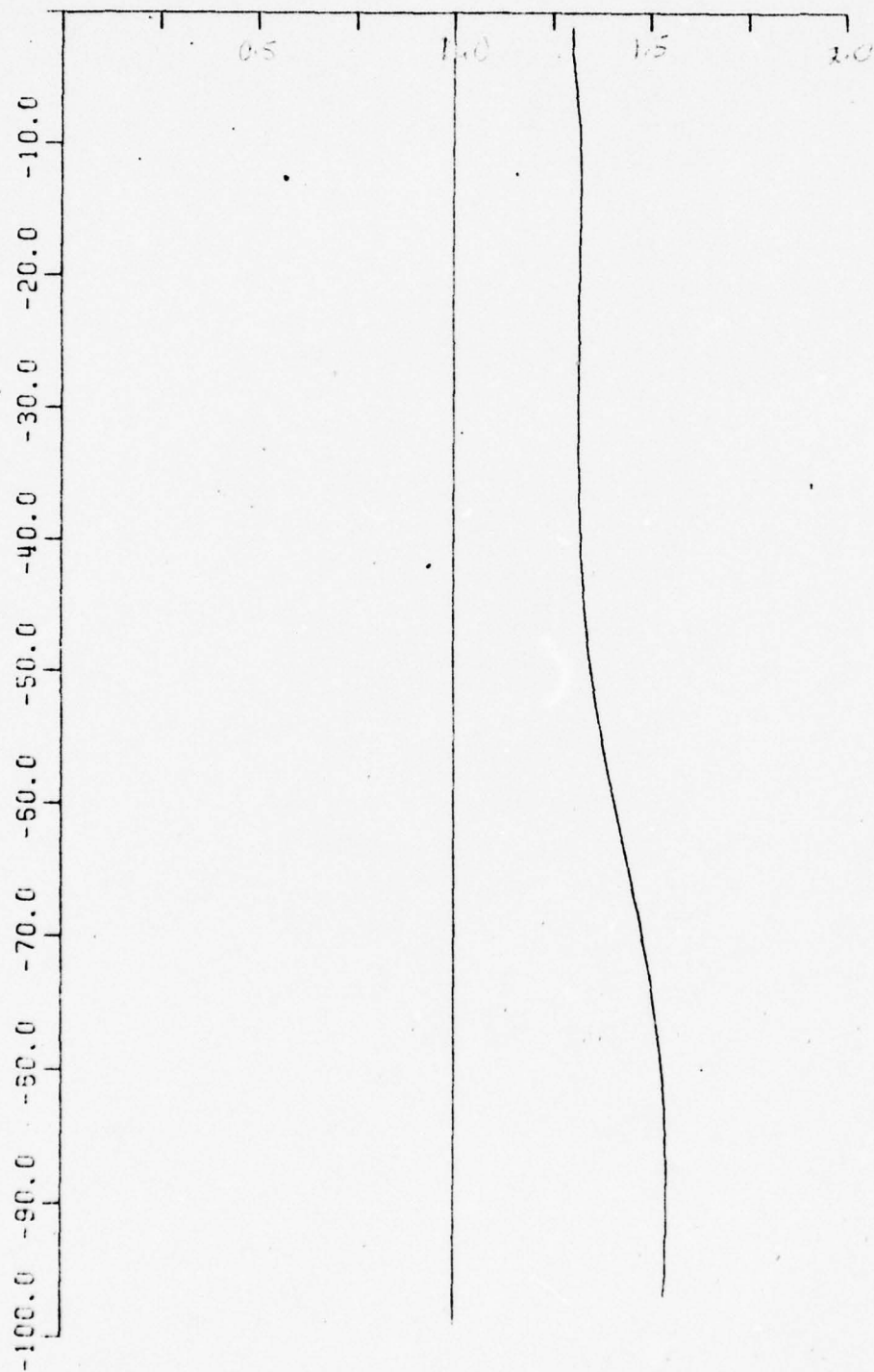


Figure IV-13. Retrieved CO<sub>2</sub> profile for Case 2.



CO2 PROFILE 2/27/75 53  
CIRCLE=T0, TRIANGLE=T0-1, PLUS=T0+1

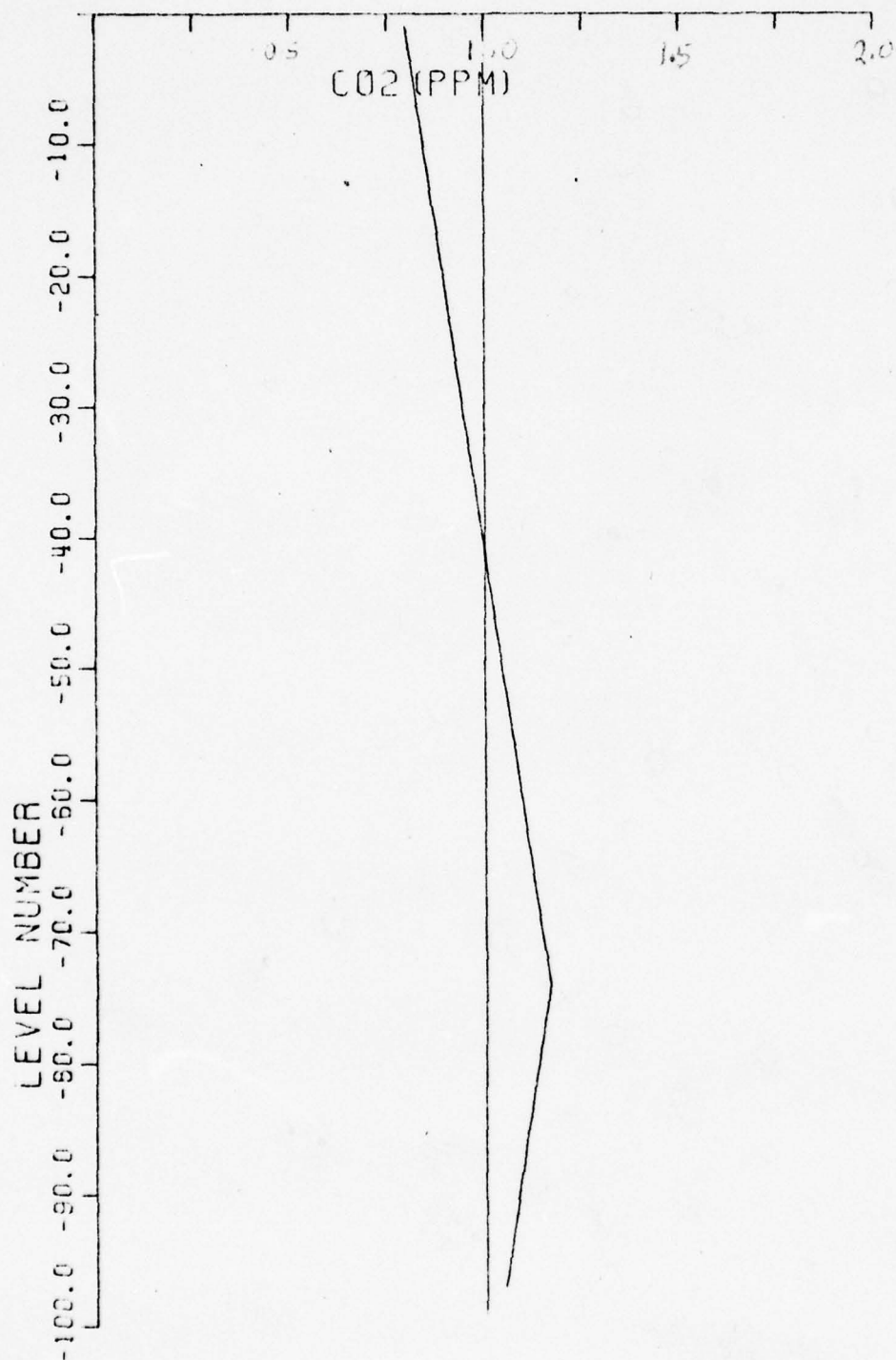


Figure IV-14. Actual CO<sub>2</sub> profile Case 3.

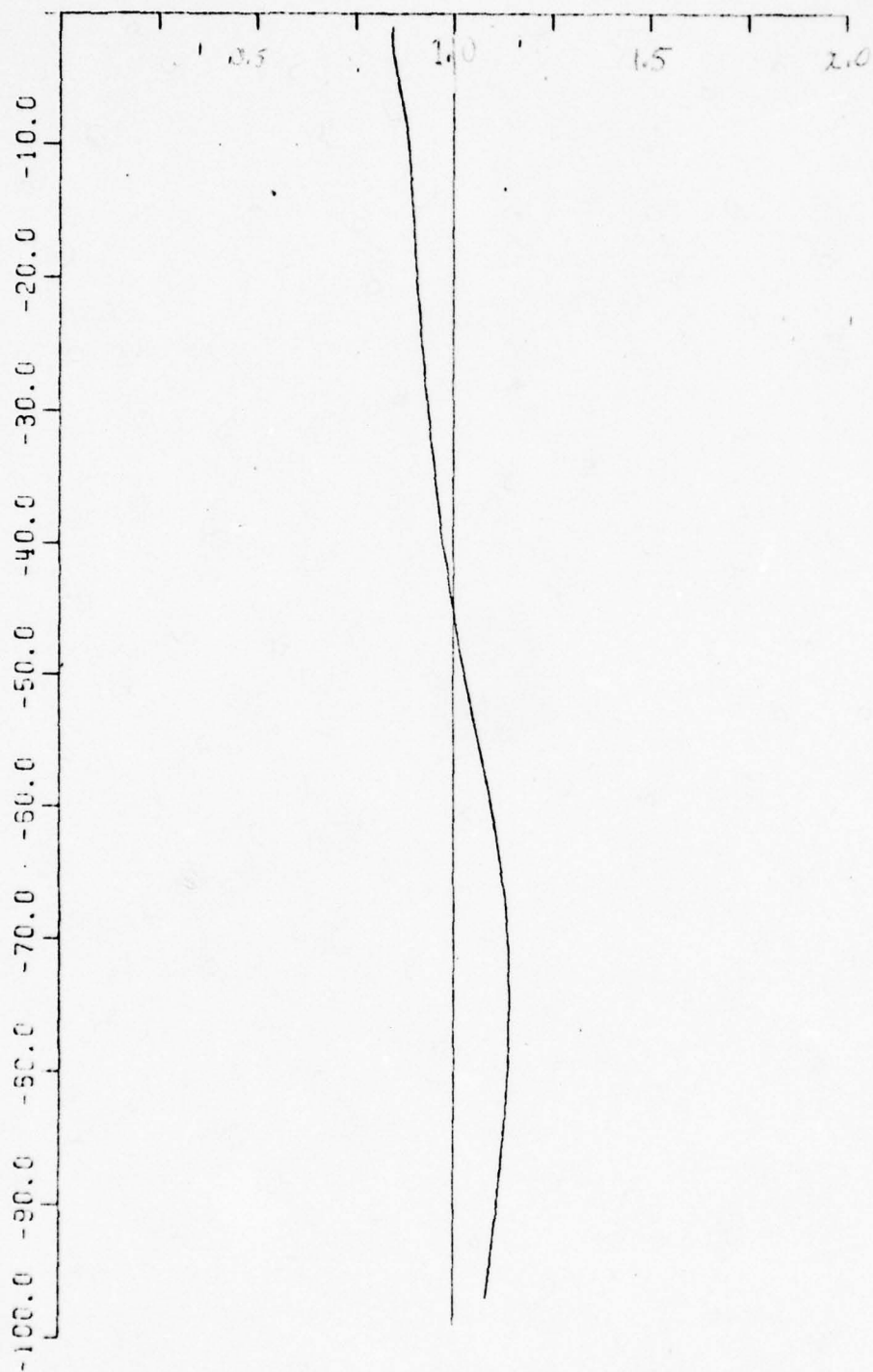


Figure IV-15. Retrieved CO<sub>2</sub> profile Case 3.

CO2 PROFILE 2/27/75 53  
CIRCLE=T0, TRIANGLE=T0-1, PLUS=T0+1

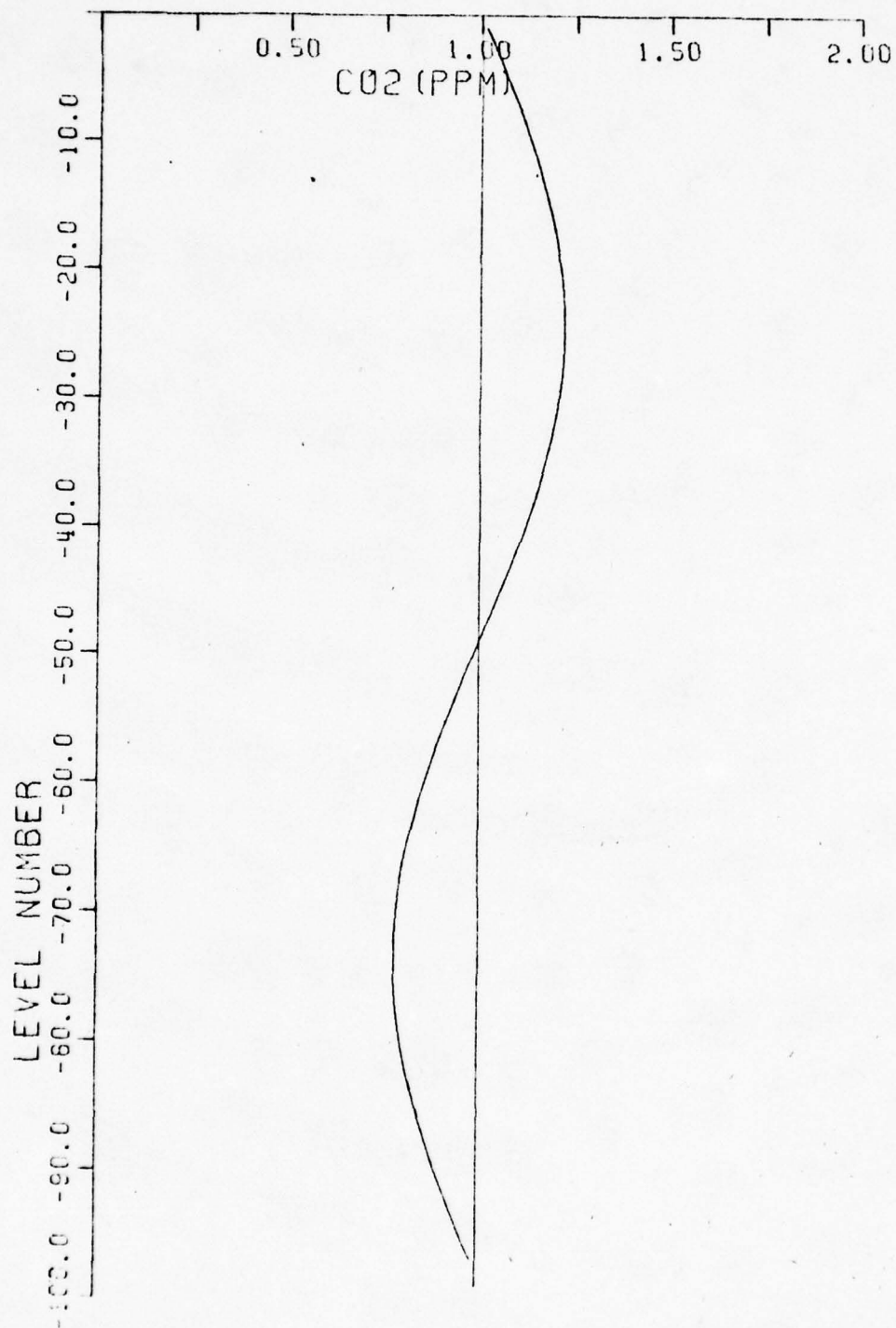


Figure IV-16. Actual CO<sub>2</sub> profile Case 4.

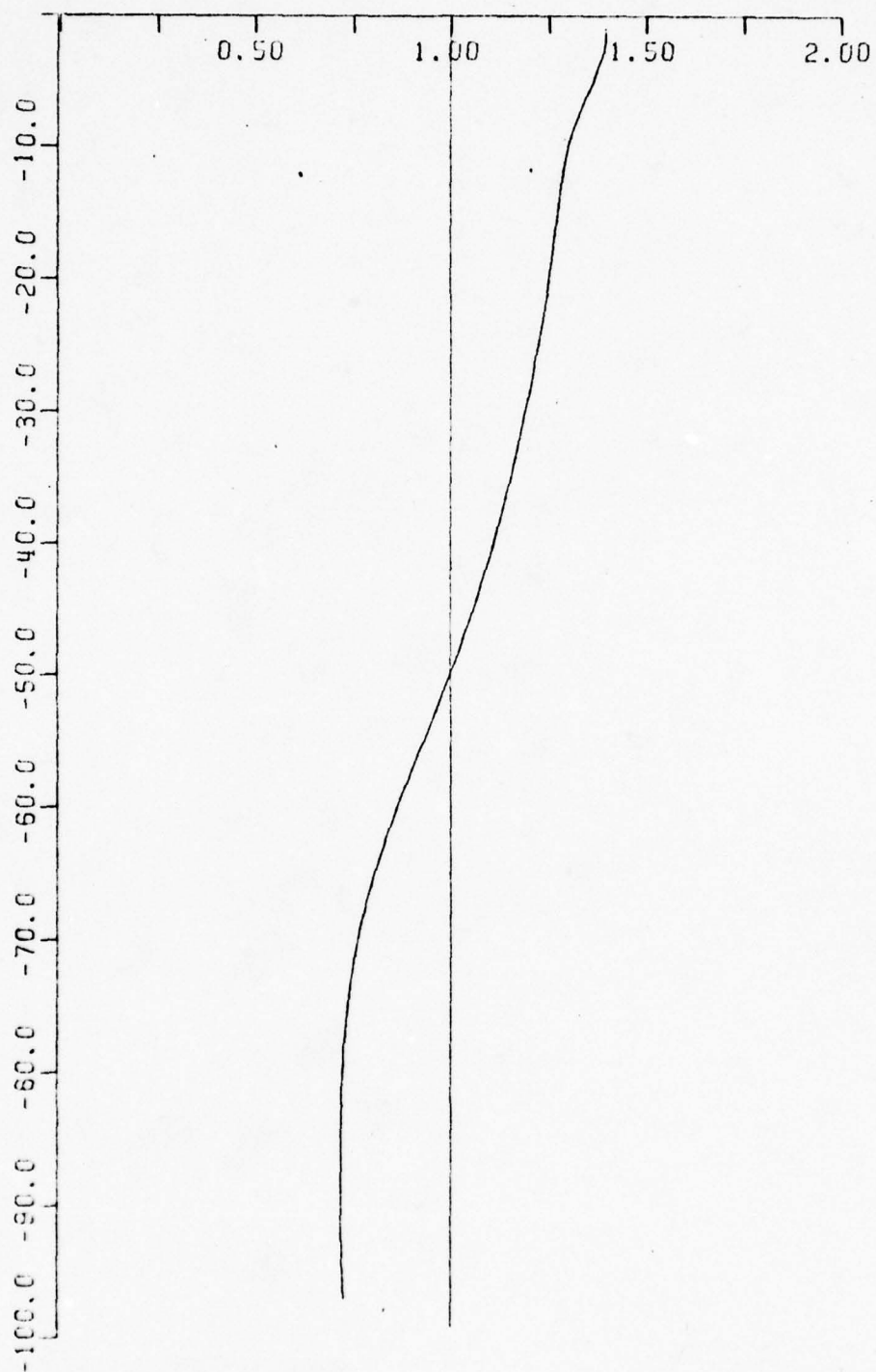


Figure IV-17. Retrieved CO<sub>2</sub> profile-Case 4.



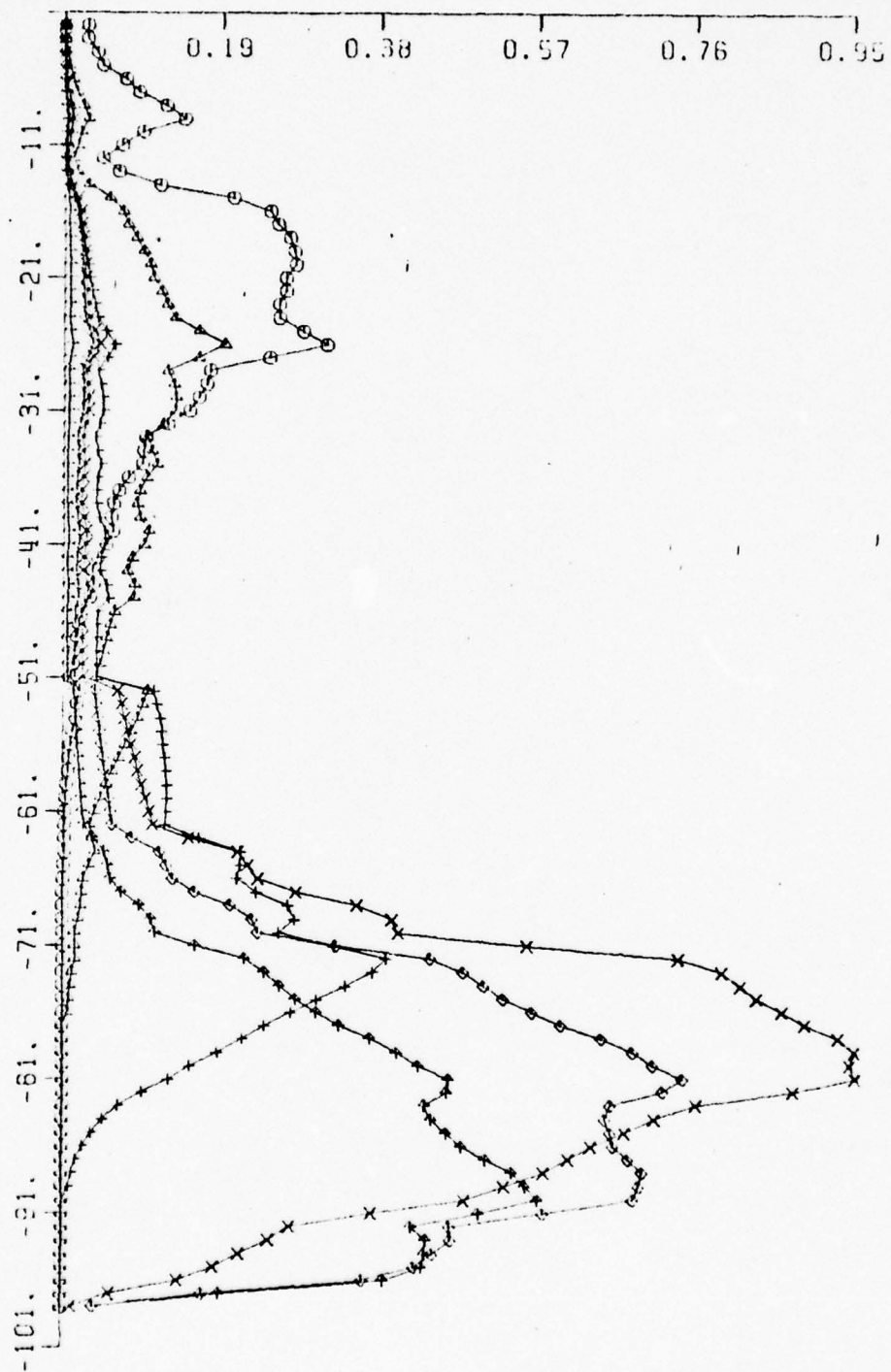


Figure IV-18. Weighting function for Case 4.  
 Circles are channel 1; triangle-2, cross-3, x-4, diamond-5 and arrow-6.

CO<sub>2</sub> PROFILE 2/27/75 53  
CIRCLE=T0, TRIANGLE=T0-1, PLUS=T0+1

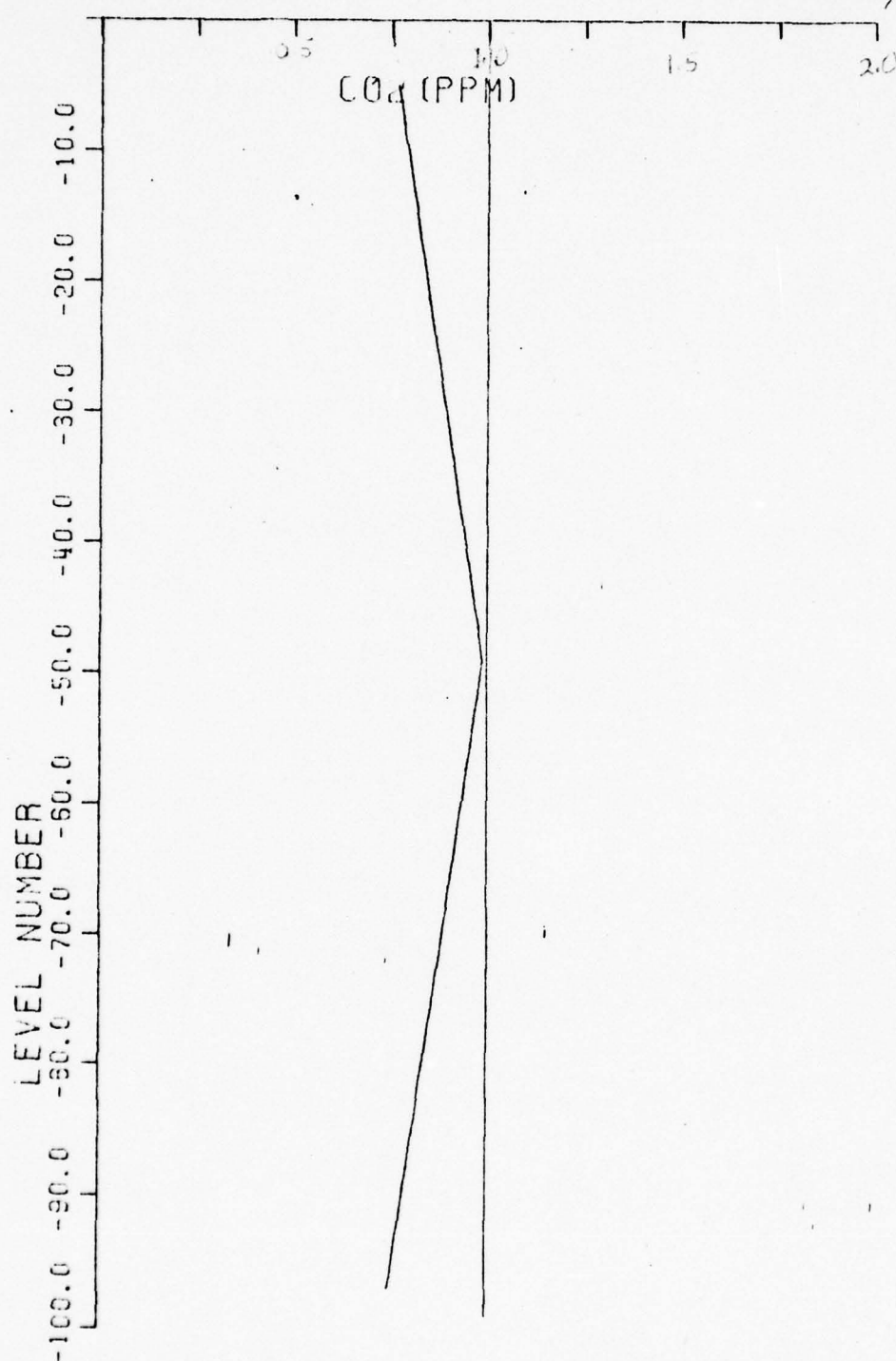


Figure IV-19. Actual CO<sub>2</sub> profile for Case 5

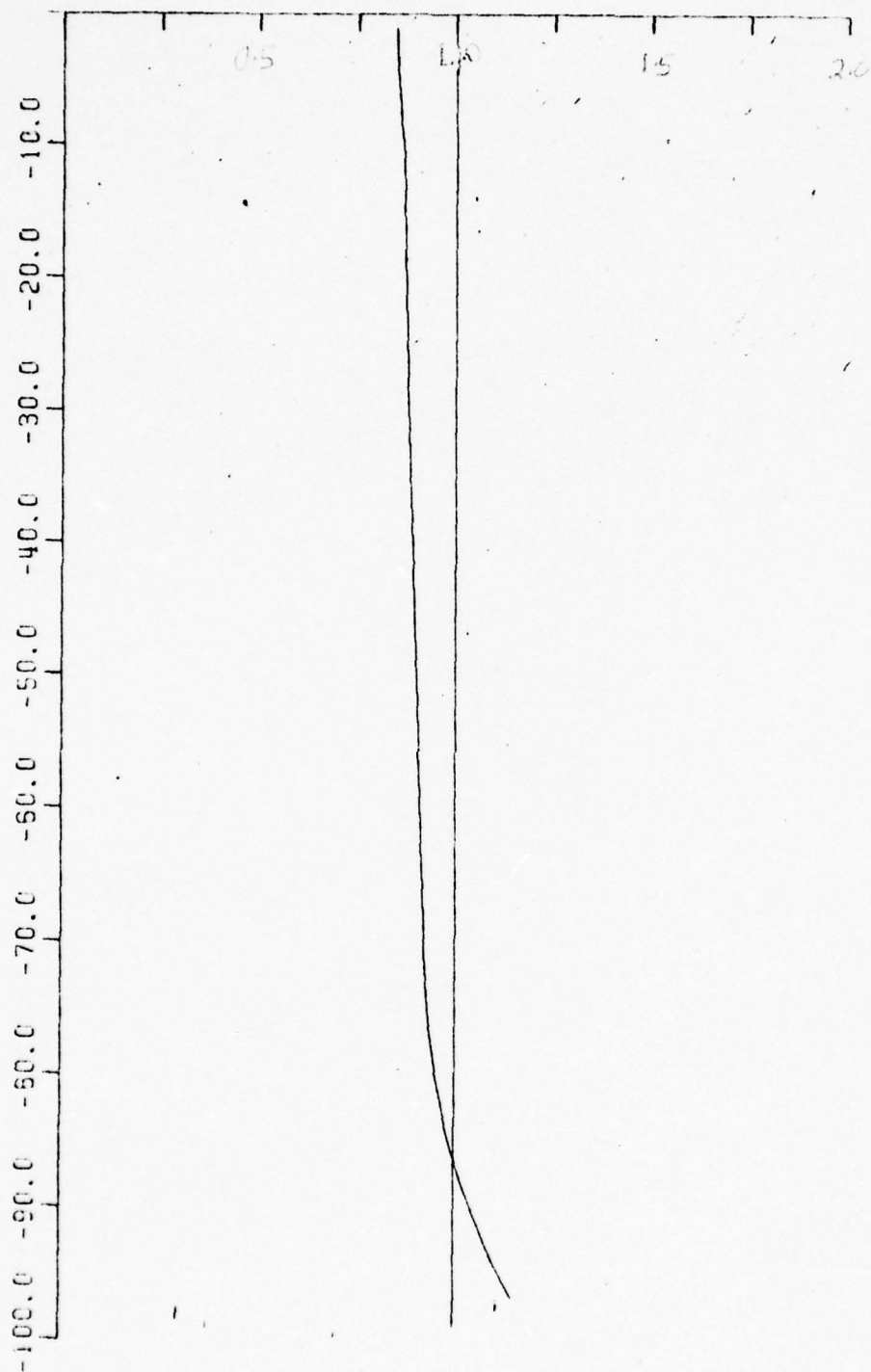


Figure IV-20. Non Converged retrieved CO<sub>2</sub> profile - Case 5

2. STUDIES AND COMPUTATIONS RELATING TO HIGH  
RESOLUTION ATMOSPHERIC TRANSMITTANCES



## 2.1 SUMMARY

Section 3.2.3 of the contract requirements called for the production of homogeneous path transmittance calculations necessary for the transmittance model work. During the course of the contract year, 400 different, filter convoluted, homogeneous path Carbon Dioxide transmittances were computed for each of the six VTPR, NOAA-2 CO<sub>2</sub> filter channels. These transmittances were computed for different CO<sub>2</sub> gas amounts for standard temperature and pressure. In addition 100 such ozone and 100 line contribution water vapor transmittances were computed for each of the first six NOAA-2 filter channels.

Section 3.2.4 called for an examination of errors resulting from the standard technique of using separate CO<sub>2</sub>, O<sub>3</sub> and H<sub>2</sub>O transmittances in the VTPR retrieval program. A preliminary line-by-line filter convoluted, transmittance calculation, for an atmosphere of 10 layers, was made utilizing H<sub>2</sub>O and CO<sub>2</sub> lines for VTPR channels 5 and 6. These two transmittances for the H<sub>2</sub>O-CO<sub>2</sub> model atmosphere were compared to the product of separate filter convoluted H<sub>2</sub>O and CO<sub>2</sub> transmittances for the same 10 layer atmosphere. For channel 5 the combined transmittance was greater than the product while for channel 6, the exact opposite result was observed. As far as this writer is concerned, there appears to be no physical or mathematical reason (other than error) to explain this result. After a considerable error search in the computer programs it was determined that the random round off error in the line-by-line computational technique was the only logical source of error. A test was made and the cumulative round off error over a 50 wave number band was determined to vary upward

to .2 wave numbers. A new program utilizing a different computational scheme for slant path calculations with considerably increased double precision summations has been written and tested. The output of this program is a magnetic tape of high resolution layered transmittance data. The second phase program of the new procedure is in the process of being tested.

This second program reads the stored data, modifies for composition variation, computes the product transmittances through the atmosphere and convolutes the data with the VTPR filters. When these programs are used the entire CO<sub>2</sub> band can be computed with an assured accuracy that each point is accurate in wavenumber to .01 cm<sup>-1</sup> (It will require more than one magnetic tape to compute an entire atmosphere with higher resolution.).

When the second program is completed, the desired calculations can be made with assurance that the random displacement of the computed line data will be eliminated.

## 2.2 CONSIDERATIONS IN HIGH RESOLUTION TRANSMITTANCES



The fundamental assumptions basic to the standard techniques used in VTPR inversions is that the atmosphere can be represented as plane parallel, in local thermodynamic equilibrium and free of scattering agents, i.e. no multiple scattering. For such an atmosphere the radiative transfer equation (RTE) has the solution (for monochromatic radiation at frequency  $\nu$ )

$$I(\nu, \theta) = B[\nu, T(p_0)] \tau(\nu, p_0, \theta) + \int_{p_0}^p B[\nu, T(p)] d\tau(\nu, p, \theta), \quad 1$$

in which the subscript 0 indicates the lower boundary, and

$p$  = pressure,

$B[\nu, T(p)]$  = Planck Function,

$\theta$  = Zenith Angle,

and

$$\tau(\nu, p, \theta) = \exp \left[ \frac{1}{g} \int_p^p k(\nu, p') q(p') \sec \theta dp' \right]. \quad 2$$

In equation 2,  $k(\nu, p)$  is the absorption coef at frequency  $\nu$  for gas  $q(p)$ .

The difficulty in VTPR retrieval is that the radiometer responds over a broad band of frequencies. Rigorously equation 1 should be convoluted with the filter band pass of the VTPR, i.e. integrated over frequency. If this were done the problem is unsolvable. Therefore, the approximation is made that the plank function can be represented by an average value: its response at a single wavenumber,  $\nu_j$ , in the bandpass interval. With this approximation the pressure and frequency integrations are interchanged and weighted transmittances are computed to replace the monochromatic transmittances:

$$\tau(\nu_j, p, \theta) = \int_{\nu_1}^{\nu_2} \tau(\nu, p, \theta) f_j(\nu) d\nu / \int_{\nu_1}^{\nu_2} f_j(\nu) d\nu, \quad 3$$

in which  $f_j(v)$  is the bandpass function (filter transmittance) and  $v_1$  and  $v_2$  are the points beyond which  $f_j(v) = 0$ . The format of equation 1 is unchanged except all terms now refer to frequency averaged values.

It is apparent that some error has been introduced into the solution of the RTE problem even before mathematical algorithms are applied to the solution. The differential elements  $d\Gamma(v_j, p, \theta)$  are defined by

$$\frac{d\tau(v, p, \theta)}{dp} = \frac{\int_{v_1}^{v_2} \frac{d\tau(v, p, \theta)}{dp} f_j(v) dv}{\int_{v_1}^{v_2} f_j(v) dv} \quad 4$$

In order to solve equation 1 in its modified form, the transmittances defined by 3 and/or 4 must be computed numerically. The next section reviews this problem.

## 2.2.2 GENERAL ASPECTS OF TRANSMITTANCE COMPUTATION TECHNIQUES

In order to numerically compute the incremental monochromatic transmittance at frequency  $\nu$  for a multicomponent gas (composition components  $\Delta q_j$ ) at temperature  $T$  and pressure  $p$  one must evaluate

$$\Delta \tau_\nu = \exp \left[ \sum_{j=1}^N \left( \sum_{i=1}^m k_{ij}[(\nu - \nu_i), T, p, q_j] \right) \Delta q_j \right], \quad 5$$

In equation 5 all absorption lines, centered at  $\nu_i$ , of each species that contribute to the absorption at frequency  $\nu$  should be included in the calculation. The absorption coefficient,  $k_{ij}$ , for the  $i^{\text{th}}$  line of the  $j^{\text{th}}$  species is a function of the pressure, temperature, frequency displacement from the line center and of the species  $q$ .

To compute the filter convoluted transmittance for a particular homogeneous path, equation 5 must be summed over all frequency points,  $\Delta \tau_\nu$ , within the filter bandpass:

$$\Delta \tau = \sum_{l=1}^{l_{\max}} \Delta \tau_{\nu_l} f(\nu_l) / \sum_{l=1}^{l_{\max}} f(\nu_l), \quad 6$$

in which the frequency points are equally spaced.

For the computation of nonhomogeneous paths (atmospheric slant paths), the transmittance to each pressure level at frequency  $\nu$  is the product of all increment transmittances for the various layers:

$$\tau(\nu, p_k) = \prod_{m=1}^k \Delta \tau_\nu(p_m) \quad 7$$

The convoluted filter transmittances (for the  $j^{\text{th}}$  filter) for each pressure level is given by

$$\tau_{\nu_j}(p_k) = \sum_{l=1}^{l_{\max}} \tau(\nu_l, p_k) f_j(\nu_l) / \sum_{l=1}^{l_{\max}} f_j(\nu_l), \quad 8$$

assuming equally spaced frequency points.

The essential differences between the computational aspects of line-by-line programs centers the line shape used and on how nonhomogeneous layers are converted to homogeneous layers.

There is little question that dopper broadening should be considered at high altitudes and that the lorentz line shape is reasonable for low altitudes. In the intermediate region, the voight line shape is the best choice of the three on purely physical grounds, however, this requires substantial increases in computer time. In addition one may incorporate collision narrowing effects.

If the lorentz shape is used, composition can be made a function of pressure and a closed analytical form can be obtained for the integral over pressure (assuming constant temperature). Other choices to convert nonhomogeneous layers to homogeneous layers is to use median values of P and T or convert to a pressure weighted mean temperature for each layer. There are several non-computational technique options available. These include the selection of lines to be included in the calculation, whose set of line parameters will be used, the number of layers in a vertical path, the extensiveness of wing contributions and the frequency density of the calculations. The availability of data usually determines whose line parameters are used. The other choices are many times determined by computer time and space considerations. For instance, the choice of low excitation energy levels for low temperature altitudes and high line strength for hotter altitudes is usually compromised by the availability of program storage space.



### 2.2.3 DATA AVAILABLE FOR CALCULATIONS AND ERROR SOURCES

All calculations made use of the "McClatchey Data Tape" for line parameter information. It is apparent that some minor errors and omissions exist in the data because even the most accurate calculations for homogeneous paths show some differences in the comparison to equivalent experimental data. Since this data is periodically upgraded, the errors and/or omissions will reduce with time.

Line-by-line calculations for the same atmospheric path computed by different agencies can vary by up to 5% (as recently reported at the Workshop on Satellite Atmospheric Soundings). This does not seem unreasonable when one considers the possible choices inherent in the calculations. It does, however, indicate considerable need for a more careful analysis of possible error sources inherent in the computational techniques. The main difficulty in evaluating the errors is the lack of usable slant path experimental data; observations over slant paths in which one has good knowledge of gas composition, temperature and pressure.

Apparently the only slant path data available are the VTPR radiance measurements obtained with simultaneous radiosonde measurements. An investigation of transmittance errors utilizing this data will by necessity, be a statistical study and also will be time consuming. For the present we can see no better or practical approach to the error problem. The new slant path computation scheme we have devised will make a study of this type somewhat easier since composition modifications can be handled much easier.

Until a detailed study of the error sources is completed we believe that working transmittances should be based upon line-by-line calculations using only doppler and lorentz profiles. The other error sources inherent in the line-by-line calculations (line parameters, wing contributions, etc.) make the added cost of voight profile computations difficult to justify. The present programs are easily changed to include other line shapes. Modifications, for test purposes, will be made to include voight profiles as specified in the error study.

### 2.3 HOMOGENEOUS PATHS

Three versions of the program outlined in Appendix 1 were used to compute  $\text{CO}_2$ ,  $\text{H}_2\text{O}$  and  $\text{O}_3$  homogeneous transmittances for the transmittance model work.

The homogeneous path program is a modification of the McClatchey program. It uses the Lorentz line shape only. The McClatchey data are read from a transfer tape which contains only the  $15\mu$  band data.

The 400  $\text{CO}_2$ , 100  $\text{H}_2\text{O}$  and 100  $\text{O}_3$  homogeneous path transmittances for each filter were computed for the following specifications:

1. Lorentz line shape only.
2. Standard Temperature and Pressure-with its implication on line selection.
3. Temperature and pressure corrections for partition function, line strength and line half-width
4. Wing contributions out to  $15 \text{ cm}^{-1}$
5. Frequency density of computed points at  $.001 \text{ cm}^{-1}$  intervals.

The program output not only gave the curve of growth for the particular filter but it also gave low resolution transmittance data covering the filter frequency band. The low resolution data was not needed.

The use of standard pressure and temperature in these calculations prevent the data being scaled directly to low temperature because the line selection would have been different for the low temperature region.

Please note that the program in Appendix 2 is still considered as a working program, unfinished, and does contain a number of nonused variables.



#### 2.4 SLANT PATH

A new computational scheme has been devised for the slant path transmittance computations. The program in Appendix B has been tested and will compute line-by-line transmittances for a layered atmosphere.

Transmittance data is generated at frequency intervals of up to  $.001 \text{ cm}^{-1}$ , averaged and placed on magnetic tape at  $.01 \text{ cm}^{-1}$  intervals. The calculations are made, for the most part, in double precision. The present scheme has eliminated the random round off errors noted in the McClatchey program and our other modifications of that program.

In its present form the Lorentz line shape only is utilized. The equivalent homogeneous, temperatures and pressures for atmospheric layers are simple median values for the layer. Temperature and/or pressure corrected half widths, line strengths and partition functions are included in the scheme. The program will cycle through a layered atmosphere; the number of layers controlled by input data.

The computational approach is to determine transmittances in two parts. The program (in Appendix 3) outputs the basic line-by-line data for the entire  $\text{CO}_2$  band region for each of the atmospheric layers. Our preliminary calculation indicates one standard magnetic tape will hold a 35 layered atmosphere with each layer containing data at  $.01 \text{ cm}^{-1}$  intervals. The second program is still under test. It reads the line-by-line data tape (up to three tapes - 3 species), computes the product transmittances through the various layers - one at a time, and convolutes the results with the various filters.

There are two main reasons for this approach:

1. The line-by-line part of the computations are the most time consuming part of the process - under the present plan the data need be

computed only once for each temperature profile.

Composition variations and different filter functions can easily be incorporated into the scheme without having to repeat the line-by-line.

2. By separating the filter convolution aspect from the program, more computer space is available for line data and other possible line shape routines.

As soon as the second program has been checked out, a completely documented report on the technique will be submitted.

APPENDIX 1



# THE EFFECT OF ATMOSPHERIC CO<sub>2</sub> VARIATIONS ON SATELLITE-SOUNDED TEMPERATURES

Rufus E. Bruce

University of Texas at El Paso  
El Paso, Texas

and

Louis D. Duncan

Atmospheric Sciences Laboratory  
US Army Electronics Command  
White Sands Missile Range, New Mexico

## 1. INTRODUCTION

An analysis has been made of the Satellite Temperature Sounding Technique (Wark and Fleming, 1966; Smith, 1970; Smith et al, 1972; Wark and Hilleary, 1969; Wark, 1970) to determine the extent of temperature errors arising from possible atmospheric CO<sub>2</sub> variations. These possible errors are compared to probable ozone-caused errors and to errors resulting from the radiometer uncertainties.

The need for the present analysis is more than academic. A recent preliminary analysis of SIRS-A data by the authors indicates non-negligible CO<sub>2</sub> variability. These findings agree with the data obtained by Gates et al (1958), in which there was evidence of a very nonuniform atmospheric CO<sub>2</sub> mixing ratio. While these results are not experimentally as satisfying as the high altitude measurements by Hagemann et al (1959), they are in general agreement with other published evidence of atmospheric CO<sub>2</sub> variability in the lower atmosphere. The measurements reported by Walter Bischof, Bert Bolin and others (see, for instance, Bischof, 1971; Bolin and Bischof, 1970) indicate variations in time-averaged CO<sub>2</sub> on the order of a few percent. Woodwell et al (1973) report substantially higher variability near ground level (125 meters). It is apparent that there is variability in the atmospheric CO<sub>2</sub> content; the only question is the amplitude of this variation. Based upon these considerations, an analysis of the effect of CO<sub>2</sub> variations on satellite-retrieved temperatures seems justified.

Two methods for evaluating the temperature errors were used. The first involves development of a closed set of equations for the approximate temperature error as a function of CO<sub>2</sub> mixing ratio deviation at particular altitudes—one different altitude for each radiometer channel. This method is based upon Chahine's (1970) analysis of the relevant radiative transfer problem. In the second method the temperature differences were evaluated from temperature profiles generated by a retrieval program in which the CO<sub>2</sub> transmittances

were modified to reflect varying CO<sub>2</sub> mixing ratios at different altitudes. The results of the first method are in reasonable agreement with the results of the more accurate second method for similar circumstances.

## 2. CLOSED SOLUTION

A closed set of equations is developed by assuming that the radiation measured by the satellite radiometer channel is related to the atmospheric parameters at and above the centroid of the transmittance weighting function. The differences between two temperature profiles are equated to the differences in the two CO<sub>2</sub> mixing ratios forming the transmittances. The atmosphere is divided into non-overlapping regions, with one region for each radiometer channel centered about the centroid of the channel's weighting function (pressure at which the weighting function is maximum). Different CO<sub>2</sub> mixing ratios are considered for each such region of the atmosphere.

For simplicity of notation the channels are ordered according to the altitude of the maximum of their weighting functions; i.e., the  $i = 1$  channel is the highest. The atmospheric regions are indexed according to the channel index.

The measured radiance,  $I_i$ , in the  $i^{\text{th}}$  channel, frequency  $\nu_i$ , is given by

$$I_i = B_i(T(P_o))\tau_i(P_o) + \int_{P_o}^{P_s} B_i(T(P)) \frac{\partial \tau_i}{\partial \ln P} d \ln P, \quad (1)$$

where  $B_i(T)$  is the Planck function,  $P$  is pressure, and  $\tau_i(P)$  is the transmittance. The subscripts  $o$  and  $s$  represent surface and satellite conditions, respectively.  $T(P)$  is the temperature obtained using the standard CO<sub>2</sub> atmospheric mixing ratio (320 ppm).

The radiative transfer equation resulting from a different CO<sub>2</sub> mixing ratio profile,  $q^*(P)$ , with transmittance  $\tau_i^*$  and temperature profile  $T^*(P)$ , is

$$I_1 = B_1[T^*(P_0)]\tau_1^* + \int_{P_0}^{P_s} B_1[T^*(P)] \frac{\partial \tau_1^*}{\partial \ln P} d \ln P. \quad (2)$$

The temperature errors,  $\Delta T_1$ , are obtained in terms of the relative deviation  $\alpha_1$  from standard in the  $CO_2$  mixing ratio by equating Eqs. (1) and (2) and expressing the quantities in the latter in terms of those in the former.

In the  $i^{th}$  interval the mixing ratio,  $q_i^*$ , is related to the standard ratio,  $q_i$ , by

$$q_i^* = (1 + \alpha_i) q_i. \quad (3)$$

The modified transmittances,  $\Delta \tau_1^*$ , in each region are expressed in terms of the standard transmittances,  $\Delta \tau_1$ , and the respective  $\alpha_1$  by

$$\Delta \tau_1^* = \Delta \tau_1 (1 + \alpha_1). \quad (4)$$

As a lower limit approximation for the effect of  $\alpha_1$ , one could replace the quantity  $(1 + \alpha_1)$  in Eq. (4) with  $1 + \alpha_1$ . Sample calculations indicate that the relationship in Eq. (4) yields more accurate results over most of the 15  $\mu m$  band atmospheric transmission profiles.

The computations of the transmittances  $\tau_1^*(P)$  and the weighting functions  $\partial \tau_1^* / \partial \ln P$  for the mixing ratio  $q^*(P)$  are shown in the Appendix.

The Planck functions are related through a first order expansion:

$$B_1[T^*(P)] = B_1[T(P)] + \frac{\partial B_1}{\partial T} \Delta T_1(P). \quad (5)$$

Substituting Eq. (5) into (2) results in

$$I_1 = \{B_1[T(P_0)] + \frac{\partial B_1}{\partial T} \Delta T(P)\} \tau_1^*(P_0) + \int_{P_0}^{P_s} \{B_1[T(P')] + \frac{\partial B_1}{\partial T} \Delta T(P')\} \frac{\partial \tau_1^*}{\partial \ln P} d \ln P. \quad (6)$$

The integrals in Eqs. (1) and (6) are evaluated according to Chahine's mean value approach:

$$\int_{P_0}^{P_s} B_1(T) \frac{\partial \tau}{\partial \ln P} d \ln P \approx B_1[T(P_1)] \frac{\partial \tau_1}{\partial \ln P} \bigg|_{P=P_1} \Delta_1 \ln P. \quad (7)$$

The integral of Eq. (6) is evaluated at the pressure at which the integrand reaches its maximum value,  $P_1$ , which is displaced from the centroid of the weighting function in Eq. (1). The equivalent width of the integrands is defined by

$$\Delta_1 \ln P = \left[ \int_{P_0}^{P_s} B_1[T(P)] \frac{\partial \tau_1}{\partial \ln P} d \ln P \right] / B_1[T(P)] \frac{\partial \tau_1}{\partial \ln P} \bigg|_{P=P_1}. \quad (8)$$

Subtracting Eq. (6) from (1), after using (7) to evaluate the integrals and rearranging terms, yields the temperature error

$$\Delta T_1(P_6) = (A_1 - F_1 + C_1 - D_1) / E_1, \quad (9)$$

in which

$$A_1 = B_1[T(P_1)] \frac{\partial \tau_1}{\partial \ln P_1} \Delta_1 \ln P_1,$$

$$F_1 = B_1[T(P_6)] \frac{\partial \tau_1^*}{\partial \ln P_6} \Delta_1 \ln P_6,$$

$$C_1 = B_1[T(P_0)] [\tau_1^*(P_0) - \tau(P_0)],$$

$$D_1 = \frac{\partial B_1(T)}{\partial T} \bigg|_{P=P_0} \tau_1^*(P_0) \Delta T_0, \text{ and}$$

$$E_1 = \frac{\partial B_1(T)}{\partial T} \bigg|_{P=P_0} \frac{\partial \tau_1^*}{\partial \ln P_8} \Delta_1 \ln P_8.$$

The subscripts 1 and 6 refer to the respective maxima of the integrands of Eqs. (1) and (6). Eq. (9) (through the  $\partial \ln \tau_1^* / \partial \ln P$  dependence) shows that the temperature error at a particular level is related not only to the modified  $CO_2$  content at the level, but also to the  $CO_2$  variations at higher levels. In practice the ground temperature error term must be determined first, since it affects the error at other levels through the factor  $D_1$ . The error determination for higher altitudes is essentially independent of the surface term.

For the purpose of illustrating Eq. (9), temperature errors resulting from uniform  $CO_2$  atmospheric variations were computed using the SIRS-B transmittances and the temperature profile shown in Figure 1. The resultant temperature errors for the  $CO_2$  relative deviations from standard of  $\pm 5\%$  and  $\pm 10\%$  are shown in Figure 2. In each case the largest error is generated in the 700- to 900-mb region and the error reverses sign above the 100-mb level.

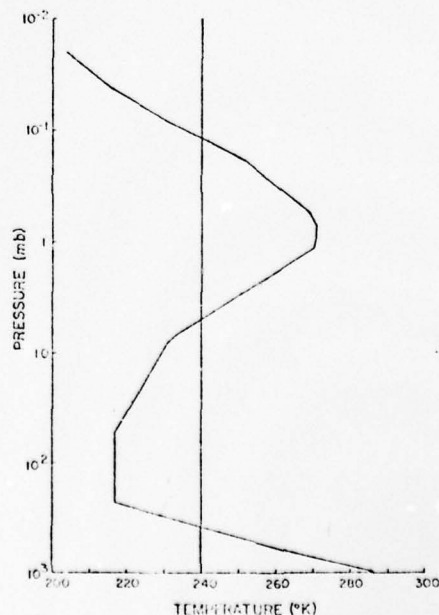


Figure 1. Temperature profile used for calculations.

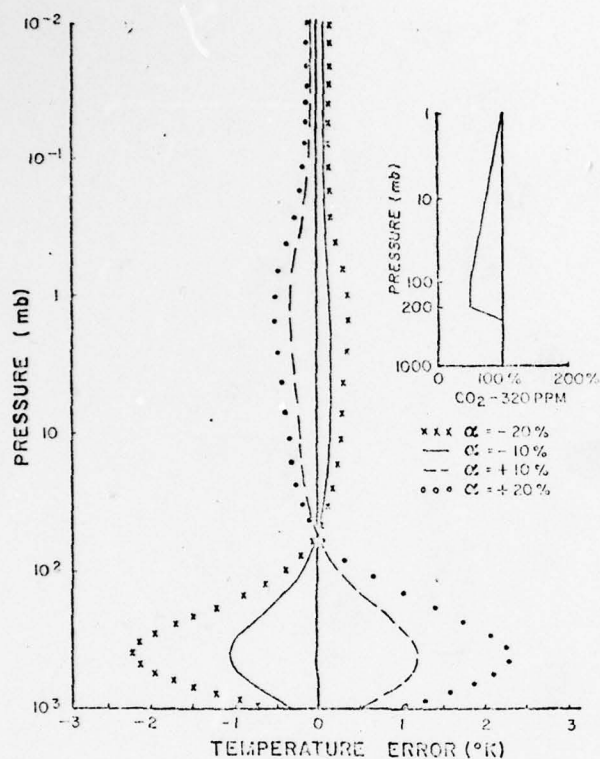


Figure 4. Retrieved temperature errors for various atmospheric  $\text{CO}_2$  deviation profiles of the family shown in the inset. a represents the maximum deviation.

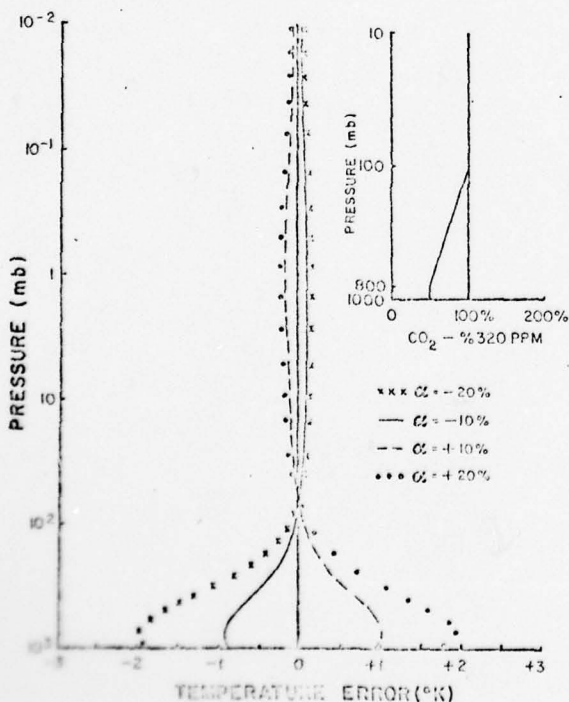


Figure 5. Retrieved temperature errors for various atmospheric  $\text{CO}_2$  deviation profiles of the family shown in the inset. a represents the maximum deviation.

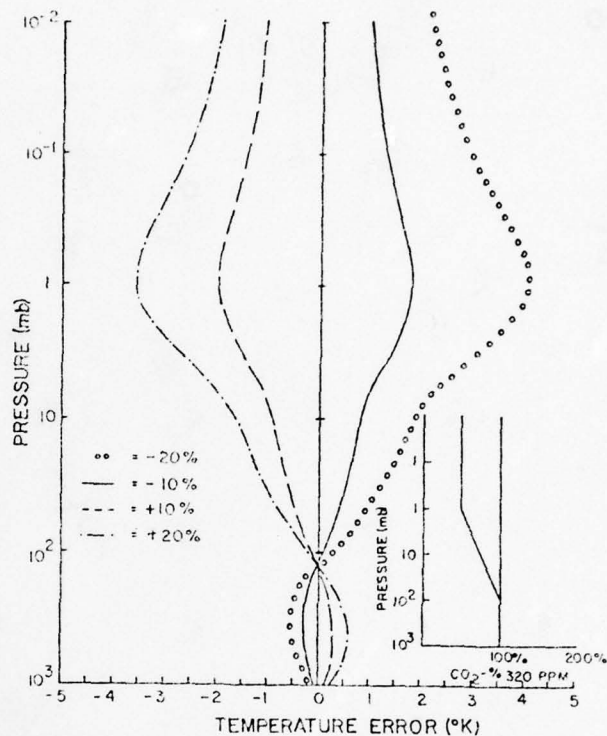


Figure 6. Retrieved temperature errors for various atmospheric  $\text{CO}_2$  deviation profiles of the family shown in the inset. a represents the maximum deviation.

#### 4. DISCUSSION

Fluctuations in the  $\text{CO}_2$  mixing ratio below the tropopause have the greatest effect on low altitude temperature errors. This follows from the fact that most of the atmospheric  $\text{CO}_2$  is below the tropopause. The temperature errors at high altitudes caused by low altitude  $\text{CO}_2$  fluctuations (Figure 4) are the result of the smoothing technique used in the retrieval program: each of the scaled constants is obtained from a weighting of all of the radiometer channel residuals (Chahine, 1971). The net result is that the computed temperature of any altitude is affected, to varying extents, by the  $\text{CO}_2$  error at any other altitude.

As an indication of the importance of  $\text{CO}_2$ -generated errors, temperature errors resulting from the use of averaged  $\text{O}_3$  profiles were calculated. Temperatures were obtained from the retrieval program in which three different ozone transmittances were used. These transmittances were for typical equatorial, polar, and averaged ozone profiles. The differences in retrieved temperatures using the average profile and that using the equatorial and the polar profiles produced an rms temperature error of  $0.3^\circ\text{K}$  when the entire profile was averaged. The average error below 500 mb was nominally  $0.8^\circ\text{K}$ , with a maximum error of about  $1^\circ\text{K}$  near ground level. As can be seen from Figure 3, a 5%  $\text{CO}_2$  variation will produce a larger temperature error.

To be of most value, statistical expected temperature errors due to  $\text{CO}_2$  fluctuations are needed. This can not be done at present because



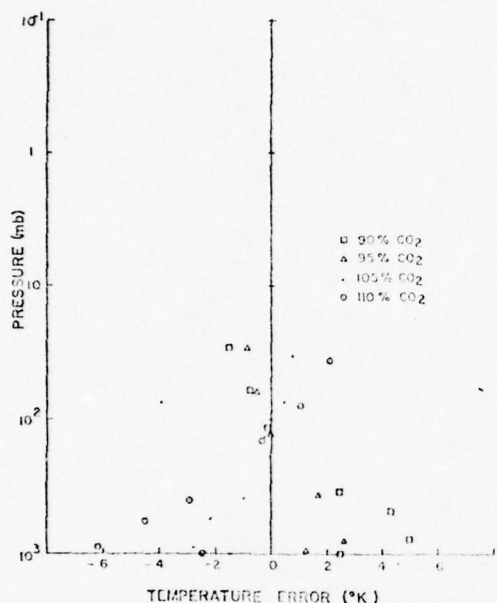


Figure 2. Temperature errors determined from Equation (10) for various uniform atmospheric  $\text{CO}_2$  concentrations.  $\text{CO}_2$  concentrations are expressed as percent of 320 ppm.

These results can be easily understood if Eq. (9) is simplified. For small  $\alpha_i$ ,

$$\frac{\partial \tau_i}{\partial \ln P_1} = \frac{\partial \tau_i}{\partial \ln P_8}$$

and

$$\Delta \ln P_1 = \Delta \ln P_8. \quad (10)$$

Expanding  $B[T(P_8)]$  in terms of  $B[T(P_1)]$ , one can obtain a lowest order approximation for the temperature error:

$$\Delta T_1 = - \left( \frac{\partial T}{\partial P} \right)_{P=P_1} (P_8 - P_1) + \dots \quad (11)$$

To a zeroth order approximation, the temperature error is simply the magnitude of the local temperature versus pressure slope times the pressure difference between the centroids of the standard and modified weighting functions. The temperature error simply results from the fact that the sensed temperature is for a different pressure than anticipated. In altitude regions with large magnitude temperature slopes, one expects large errors; where small slopes exist, one expects proportionally smaller errors. The error changes sign with the change of slope.

It should be noted that Eq. (10) may be utilized to examine the temperature error resulting from any absorber perturbation. One need only use the correct combination of individual transmittances to correctly specify the total transmittance.

### 3. RETRIEVAL METHOD

The second method utilized synthetic data in a temperature retrieval program for the SIRS-B satellite temperature sounding technique (Duncan, 1973). The transmittances were modified for arbitrary  $\alpha_i(P)$ , and the errors between the retrieved temperature (for the modified  $\text{CO}_2$  content) were subtracted from the standard. The results of this technique are shown in Figure 3 and may be compared to the results of Eq. (10) (Figure 2). Uniform  $\alpha_i$  of  $\pm 5\%$  and  $\pm 10\%$  was used in the retrieval program. As can be seen, the agreement with the closed equation solution is generally good.

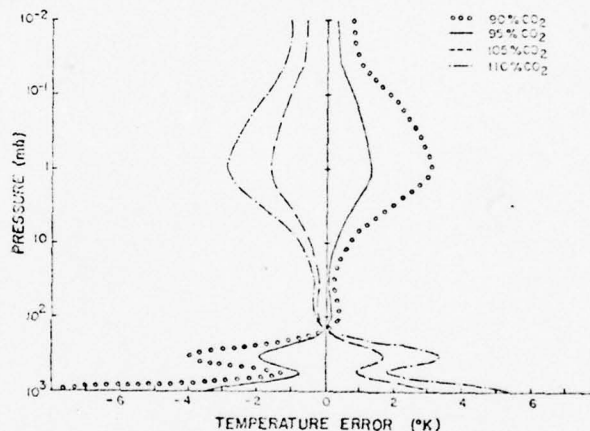


Figure 3. Temperature error versus altitude for different uniform atmospheric  $\text{CO}_2$  concentrations determined by the retrieval program. The  $\text{CO}_2$  concentrations are expressed as percent of 320 ppm.

The expected temperature errors for various  $\text{CO}_2$  modification profiles are shown in Figures 4 through 6. On each graph the  $\text{CO}_2$  variation is shown. The parameter  $\alpha$  on the temperature error curves represents the maximum  $\text{CO}_2$  deviation for the particular family of  $\text{CO}_2$  deviation profiles. For example, in Figure 4,  $\alpha$  represents the  $\text{CO}_2$  change in the 800- to 1000-mb region. In the range from 800 mb to 100 mb,  $\alpha$  reduces linearly from its value at 800 mb to 0 at 100 mb. The  $\Delta T$  curves are for the particular  $\alpha$  chosen. In the other figures,  $\alpha$  and the graphs are similarly related.



the amplitude of probable  $\text{CO}_2$  variations is not known. The use of the variations in monthly averages or the variances measured at ground level seem equally invalid. One can, however, compare a 5%  $\text{CO}_2$  fluctuation temperature error to that caused by the radiometer random error. The reported random error of  $0.25 \text{ erg sec}^{-1} \text{ cm}^{-2} \text{ sec}^{-1} \text{ cm}$  (Wark and Hilleary, 1969), which when averaged over a given locality is substantially less (Fritz, 1970), produces direct rms temperature errors of the order of  $0.5^\circ\text{K}$ . It is clear from the figures that a 5%  $\text{CO}_2$  uncertainty has a larger associated error in the lower atmosphere. It might be noted that if one used the lower limit approximation,  $\tau_i^* = \tau_i \sqrt{1 + \alpha_i}$ , the basic conclusions are unchanged.

Based upon these results, one can speculate that a contributor to the difficulties in equating experimental and theoretical  $15\text{-}\mu\text{m}$  atmospheric transmittances can be a variation in the  $\text{CO}_2$  content. This is not to say that aerosols or computational techniques are not a problem, but that one should consider the possibility of some uncertainty in  $\text{CO}_2$ . One can equally speculate that some of the problems in temperature retrievals rest on the same cornerstone.

Acknowledgement. The authors gratefully acknowledge the comments and criticisms of Dr. D. Q. Wark.

#### REFERENCES

- Bischof, W., 1971: Carbon Dioxide Concentration in the Upper Troposphere and Lower Stratosphere. II. *Tellus XXIII*, 6, 558.
- Bolin, B., and W. Bischof, 1970: Variation of the Carbon Dioxide Content of the Atmosphere in the Northern Hemisphere. *Tellus XXII*, 4, 431.
- Chahine, M. T., 1970: Inverse Problems in Radiative Transfer: Determination of Atmospheric Parameters. *J. of Atmos. Sci.*, 6, 27, 960.
- , 1971: A General Relaxation Method for Inverse Solution of the Full Radiative Transfer Equation. *J. of Atmos. Sci.*, 5, 29, 741.
- Duncan, L. D., 1973: An Iterative Inversion of the Radiative Transfer Equation for Temperature Profiles. ECOM 5534. Atmospheric Sciences Laboratory, White Sands Missile Range, NM.
- Fritz, S., 1970: Earth's Radiation to Space at 15 Microns: Stratospheric Temperature Variations. *J. of Appl. Meteor.*, 9, 815.
- Gates, D. M., D. G. Murclay, C. C. Shaw and R. J. Herbold, 1958: Near Infrared Solar Radiation Measurements by Balloon to an Altitude of 100,000 Feet. *J. of Optical Soc. of Amer.*, 12, 48, 1010.
- Hagemann, F., J. Gray, Jr., L. Machta and A. Turkevich, 1959: Stratospheric Carbon - 14, Carbon Dioxide, and Tritium. *Science*, 130, 542.
- Smith, W. L., 1970: Iterative Solution of the Radiative Transfer Equation for the Temperature and Absorbing Gas Profile of an Atmosphere. *Appl. Optics*, 9, 1933.
- , H. M. Woolf and H. E. Fleming, 1972: Retrieval of Atmospheric Temperature Profiles from Satellite Measurements for Dynamical Forecasting. *J. of Appl. Meteor.*, 11, 133.

- Wark, D. Q., 1970: SIRS: An Experiment to Measure the Free Air Temperature from a Satellite. *Appl. Optics*, 8, 9, 1761.
- , and H. E. Fleming, 1966: Indirect Measurements of Atmospheric Temperature Profiles from Satellites. *Mon. Wea. Rev.*, 6, 94, 351.
- , and D. T. Hilleary, 1969: Atmospheric Temperature: Successful Test of Remote Probing. *Science*, 165, 1256.
- Woodwell, G. M., R. A. Houston and N. R. Tempel 1973: Atmospheric  $\text{CO}_2$  at Brookhaven, Long Island, New York: Patterns of Variation Up to 125 Meters. *J. of Geophys. Res.*, 6, 78, 932.

#### APPENDIX

Let  $\tau_i(P)$  be the transmittance, at frequency  $\nu_i$ , determined for a standard  $\text{CO}_2$  atmospheric mixing ratio (320 ppm). It is desired to determine the transmittance for a different  $\text{CO}_2$  mixing ratio profile  $q^*(P)$ . The relative deviations from standard are

$$\alpha_i(P) = q^*(P)/q(P) - 1. \quad (\text{A1})$$

Denote by  $P_1 < P_2 < \dots < P_n$  the values for  $P$  for which  $\tau_i(P)$  are known. The modified transmittances  $\Delta\tau_{ij}^*$  for the pressure layer  $(P_{j-1}, P_j)$  can be expressed in terms of the standard transmittances,  $\Delta\tau_{ij}$ , by

$$\Delta\tau_{ij}^* = \Delta\tau_{ij}^{(1+\bar{\alpha}_j)}, \quad (\text{A2})$$

where  $\bar{\alpha}_j$  is the mean value of  $\alpha(P)$  over the layer.

Sample calculations indicate that the relationship in Eq. (A2) is a reasonable approximation for the  $15\text{-}\mu\text{m}$  transmittances. Expressing the modified total transmittance in terms of Eq. (A2),

$$\tau_i^*(P_j) = \prod_{P_k < P_j} \Delta\tau_{ik}^* = \prod_{P_k < P_j} \Delta\tau_{ik}^{(1+\bar{\alpha}_k)}; \quad (\text{A3})$$

This allows the modified weighting functions to be evaluated:

$$\left. \frac{\partial \tau_i^*}{\partial \ln P} \right|_{P=P_j} = \left( \prod_{P_k < P_j} \Delta\tau_{ik}^{(1+\bar{\alpha}_k)} \right) \left( \sum_{P_k < P_j} \frac{(1+\bar{\alpha}_k) \partial \Delta\tau_{ik}}{\Delta\tau_{ik} \partial \ln P} \right) \bigg|_{P=P_k} \quad (\text{A4})$$

or

$$\left. \frac{\partial \tau_i^*}{\partial \ln P} \right|_{P=P_j} = \tau_i^*(P) \left\{ \sum_{P_k < P_j} (1+\bar{\alpha}_k) \frac{\partial \ln \Delta\tau_{ik}}{\partial \ln P} \right\} \bigg|_{P=P_k} \quad (\text{A5})$$

APPENDIX 2

Homogeneous Transmittance Program

```

DIMENSION W(7), R(325), GNU(3000), S(3000), ALPHA(3000), EDP(3000)
DIMENSION MOL (3000), CAY1(7), OPD(6000), FNU(1000), TRANS(1000)
DIMENSION SUM1(7), CS2(7)
DIMENSION XNU(325), WX(100), FSUM(100)
DIMENSION WW(100)
DIMENSION QV(7,7), TQV(7), QVF(7)
DOUBLE PRECISION CAY1, SUM1
C THIS PROGRAM GENERATES A TRANSMITTANCE SPECTRUM WITH OUTPUT RESULTS
C PRINTED EVERY DELV WAVE NUMBERS BETWEEN THE INITIAL FREQUENCY,
C V1, AND THE FINAL FREQUENCY, V2. CALCULATIONS ARE PERFORMED FOR
C A UNIFORM, CONSTANT PRESSURE, CONSTANT TEMPERATURE PATH CONTAINING
C ANY OR ALL OF THE MOLECULAR SPECIES DESCRIBED IN THIS REPORT
C IN ARBITRARY AMOUNTS. MOLECULAR ABUNDANCES MUST BE SPECIFIED
C IN THE UNITS (MOLECULES/CM2). MONOCHROMATIC CALCULATIONS ARE
C MADE AT FREQUENCY INTERVALS, DV, AND A TRIANGULAR SLIT FUNCTION
C OF HALF-WIDTH, A, IS CONVOLVED WITH THE MONOCHROMATIC RESULTS
C
C
C
C
C DEPTH=0.001
C PI=3.14159
C DO 864 M=1,7
864 READ (5,862)(QV(M,I),I=1,7)
862 FORMAT(7F10.5)
C TQV(1)=175.
C DO 863 I=2,7
863 TQV(I)=TQV(I-1)+25.
C TQV(6)=296.
C IRUN=0
1015 CONTINUE
C IRUN=IRUN+1
C IEOF=0
C KEND=0
C SUM=0.0
C IV=1
C READ(5,305)IR,KENDF
C DO 306 I=1,IR
306 READ(5,307)CODE,XNU(I),R(I)
305 FORMAT(2I5)
307 FORMAT(F10.4,F10.1,F10.5)
C
C READ INPUT PARAMETERS (P=PRESSURE), (T=TEMPERATURE),
C W(1)=H2O, W(2)=CO2, W(3)=O3, W(4)=N2O, W(5)=CO, W(6)=CH4, W(7)=O2.
C V1 AND V2 ARE FREQUENCY LIMITS FOR WHICH OUTPUT RESULTS ARE REQUIRED.
C DV IS MONOCHROMATIC FREQUENCY INCREMENT.
C BOUND IS THE FREQUENCY FROM ANY LINE CENTER BEYOND WHICH THE LINE
C WILL BE NEGLECTED.
C A IS THE HALF-WIDTH OF A TRIANGULAR SLIT FUNCTION.
C DELV IS FREQUENCY INCREMENT OF CONVOLVED OUTPUT TRANSMITTANCE
C RESULTS.
C
C READ(5,85)V1,V2,DV,BOUND,A,DELV
C PRINT 87,V1,V2,DV,BOUND,A,DELV
C V10=V1
C IF(A*2/DV+1.GT.3000) CALCULATION CANNOT BE DONE
C IF THERE ARE MORE THAN 3000 LINES READ FROM TAPE IN A FREQUENCY RANGE

```



```

C      OF 2(A+BOUND) CALCULATION CANNOT BE DONE
      VBOT=V1-A-BOUND
      VTOP=V2+A+BOUND
      I=1
      ILL=1
1      READ(2,95)GNU(I),S(I),ALPHA(I),EDP(I),IDAT,ISOT,MOL(I)
      IF(GNU(I).LT.VBOT)GO TO 1
      IF(GNU(I).GT.VTOP)GO TO 11
      IF(MOL(I).NE.3) GO TO 1
      IF(I.GT.2999)GO TO 11
      I=I+1
      GO TO 1
11     I1=1
      READ(5,77)P,T
      PRINT 79, P,T
      READ(5,81)(W(M),M=1,7)
      PRINT 83
      PRINT 81, (W(M),M=1,7)
      DO 304 M=1,7
304    W(M)=W(M)*2.69E+19
      PRINT 700,(W(M),M=1,7)
700    FORMAT(14H W IN MOL/CM2,7(2X,E12.6))
C      SET WX VALUES (MULTIPLES OF THE W(I) VALUES)
      WX(1)=1.0
      DO 1000 K=2,100
1000   WX(K)=WX(K-1)+5.0
      DO 1000 CONTINUE
      MIN=0
      DO 870 M=2,7
870    MIN=MIN+1
      IF(T.LE.TQV(M))GO TO 871
871    DQV=(T-TQV(MIN))/(TQV(MIN+1)-TQV(MIN))
      DO 869 M=1,7
869    QVF(M)=(QV(M,MIN)+(DQV*(QV(M,MIN+1)-QV(M,MIN))))/QV(M,6)
      KEND=KEND+1
      DO 1003 K=1,100
1003   FSUM(K)=0.0
      FSUM1=0.0
      PRINT 97, VBOT,VTOP,GNU(I1),I1
      I5=1
      V2P=GNU(I1)-BOUND-A
C
C      TAPE HAS BEEN READ FOR ALL NECESSARY LINES OR FOR THE MAXIMUM NO.
C      OF LINES POSSIBLE SUBJECT TO RECYCLING.
C      HALFWIDTHS WILL BE SUPPLIED BELOW WHEN THEY DO NOT APPEAR
C      ON TAPE.
C
      DO 15 I=ILL,I1
      M=MOL(I)
      IF (M.EQ.1) GO TO 15
      IF (ALPHA(I).GT.0.0) GO TO 13
      IF (M.EQ.2) ALPHA(I)=0.07
      IF (M.EQ.3) ALPHA(I)=0.11
      IF (M.EQ.4) ALPHA(I)=0.08
      IF (M.EQ.5) ALPHA(I)=0.06
      IF (M.EQ.6) ALPHA(I)=0.055

```



```

114.      IF (M.EQ.7) ALPHA(I)=0.048
115.      13  IF (ALPHA(I).LT.0.01.OR.ALPHA(I).GT.1.0) ALPHA(I)=0.06
116.      C
117.      15  CONTINUE
118.      IS=1
119.      P0=1013.00
120.      T0=296.00
121.      CS1=(T0-T)/(T0*T*0.6946)
122.      C
123.      C  ROTATIONAL PARTITION FUNCTION IS DEFINED BELOW
124.      C
125.      DO 21 M=1,7
126.      IF (M.EQ.1) GO TO 17
127.      IF (M.EQ.2) GO TO 19
128.      IF (M.EQ.3) GO TO 17
129.      IF (M.EQ.4) GO TO 19
130.      IF (M.EQ.5) GO TO 19
131.      IF (M.EQ.6) GO TO 17
132.      IF (M.EQ.7) GO TO 19
133.      17  CS2(M)=((T0/T)**1.5)
134.      GO TO 21
135.      19  CS2(M)=T0/T
136.      21  CONTINUE
137.      CA=((T0/T)**0.5)*(P/P0)
138.      C
139.      C  TEMPERATURE DEPENDENCE OF ALL LINE INTENSITIES COMPUTED HERE.
140.      C
141.      V=V1-A
142.      25  DO 27 M=1,7
143.      CAY1(M)=0.0
144.      27  SUM1(M)=0.0
145.      C
146.      C  DETERMINE INDICES (15 AND 16) INDICATING WHICH SPECTRAL LINES
147.      C  ARE TO BE USED IN THE CALCULATION AT FREQUENCY V.
148.      C
149.      DO 33 I=15,11
150.      IF (V-BOUND-GNU(I)) 29,29,33
151.      29  IS=1
152.      GO TO 35
153.      33  CONTINUE
154.      IS=11
155.      GO TO 49
156.      35  DO 39 J=15,11
157.      IF (V+BOUND-GNU(J)) 37,37,39
158.      37  I6=J-1
159.      GO TO 43
160.      39  CONTINUE
161.      I6=11
162.      C
163.      C  COMPUTE THE OPTICAL DEPTH AND TRANSMITTANCE AT FREQUENCY V.
164.      C
165.      43  DO 45 I=15,16
166.      M=MOL(I)
167.      Z=ABS(V-GNU(I))
168.      X1=S(I)*CS2(M)*EXP(-EDP(I)*CS1)*QVF(M)
169.      X2=ALPHA(I)*CA
170.      SUM1(M)=X1*X2/(Z**2+X2**2)

```

```

      CAY1(M) =CAY1(M)+SUM1(M)
45  CONTINUE
      CAY=0.0
      DO 47 M=1,7
47  CAY=CAY+CAY1(M)*W(M)
      OPD(IV)=CAY*0.3183
      GO TO 51
49  OPD(IV)=0.0
51  OPD(IV)=EXP(-OPD(IV))
      IF(V.GT.XNU(IR))GO TO 338
335 IF(V.GE.XNU(IF).AND.V.LE.XNU(IF+1))GO TO 337
      IF(V.GT.XNU(IF+1))GO TO 336
      IF(V.LT.XNU(IF))IF=IF-1
      GO TO 335
336 IF=IF+1
      GO TO 335
337 DRF=R(IF)+(V-XNU(IF))*(R(IF+1)-R(IF))/(XNU(IF+1)-XNU(IF))
      DO 1001 K=1,100
1001 FSUM(K)=FSUM(K)+ DRF*(OPD(IV)*WX(K))
      FSUM1=FSUM1+DRF
      GO TO 339
338 WRITE(6,340)V
340 FORMAT(5X,9HNO ADD,V=,E14.6)
339 CONTINUE
      IF ((V+DV).GT.V2P) GO TO 53
      IF (V.GE.V2+A) GO TO 53
      IF (IV.GE.6000) GO TO 53
      IV=IV+1
      V=V+DV
      GO TO 25

```

C  
 C AT THIS POINT, CYCLE BACK TO STATEMENT 25 AND COMPUTE THE  
 C MONOCHROMATIC TRANSMITTANCE AT V+DV, ETC.  
 C IF STATEMENT 53 IS REACHED, ALL POSSIBLE MONOCHROMATIC TRANSMITTANCE  
 C VALUES HAVE BEEN COMPUTED, AND THE SLIT FUNCTION CONVOLUTION WILL  
 C NOW BE PERFORMED IN LOOP 57

```

53  FREQ=V1
      PRINT 101, IV,V,V2P
      WRITE OUT TRANSMISSIONS, MONOCHROMATIC
      WRITE(6,201)(OPD(L2),L2=1,IV)
201  FORMAT(10F12.8)
      FINAL=V1+6000.*DV-A-DELV
      V=V1-A
      JFNU=1
      L=DELV/DV+0.01
      IA=1
55  SUM=0.0
      SUM2=0.0
      DO 57 I=IA,IV
      SUM=SUM+(A-ABS(V-FREQ))*OPD(I)
      SUM2=SUM2+(A-ABS(V-FREQ))
      V=V+DV
      IF (V-(FREQ+A)) 57,59,59
57  CONTINUE
59  TRANS(JFNU)=SUM/SUM2
      FNU(JFNU)=FREQ

```

```

28. IF (FREQ.GT.V2) GO TO 61
29. IF (FREQ.GT.V2P) GO TO 61
30. IF (FREQ.GE.FINAL) GO TO 61
31. FREQ=FREQ+DELV
32. IF (JFNU.GE.1000) GO TO 61
33. JFNU=JFNU+1
34. IA=IA+L
35. V=FREQ-A
36. SUM=0.0
37. GO TO 55
38. C
39. C CONVOLVED TRANSMITTANCE RESULTS ARE NOW PRINTED OUT.
40. C
41. 61 PRINT 103, JFNU
42. PRINT 104
43. PRINT 105, (FNU(J),TRANS(J),J=1,JFNU)
44. IF (FREQ.GE.V2) GO TO 75
45. IF (FREQ.GT.V2P) GO TO 67
46. IF (JFNU.GE.1000) GO TO 65
47. IF (FREQ.GE.FINAL) GO TO 63
48. GO TO 75
49. 63 V1=FINAL+DELV
50. IS=1
51. IV=1
52. JFNU=1
53. V=V1-A
54. GO TO 25
55. 65 IA=IA+L
56. C
57. C IF STATEMENT 65 IS REACHED, ADDITIONAL MONOCHROMATIC CALCULATIONS
58. C ARE REQUIRED TO SATISFY THE TOTAL FREQUENCY RANGE OVER WHICH
59. C CONVOLVED RESULTS ARE REQUIRED.
60. C
61. JFNU=1
62. V=FREQ-A
63. GO TO 55
64. 67 IV=1
65. C
66. C IF STATEMENT 67 IS REACHED, THE DATA FROM THE DATA TAPE WILL BE
67. C REORGANIZED AND THE TAPE WILL BE READ AGAIN.
68. C
69. JFNU=1
70. V1=FREQ
71. VBOT=V1-A-BOUND
72. DO 69 IN =1,11
73. IF (GNU(IN).GT.VBOT) GO TO 71
74. 69 CONTINUE
75. IN=11
76. 71 IJ=IN
77. L=1
78. DO 73 I=1J,11
79. GNU(L)=GNU(I)
80. S(L)=S(I)
81. ALPHA(L)=ALPHA(I)
82. EDP(L)=EDP(I)
83. MOL(L)=MOL(I)
84. 73 L=L+1

```



```

      I=L
      ILL=L
      GO TO 1
75  CONTINUE
      DO 1004 K=1,100
      FSUM(K)=FSUM(K)/FSUM1
      WU=W(3)*WX(K)/2.69E19
      WW(K)=WU
      WRITE(6,341)CODE,P,T,WU,FSUM(K)
1004 CONTINUE
      WRITE(7,2002)(WW(K),K=1,100)
2002 FORMAT(8F10.5)
      WRITE(7,2003)(FSUM(K),K=1,100)
2003 FORMAT(8F10.7)
341  FORMAT(30H 03 UNIFORM TRANS. FOR INST.,F10.4,13H AT PRESSURE ,F8
      1.3,10H AND TEMP.,F8.3,12H 03 ATMCN.,F9.5,11H TRANSMIT.,E15.8)
      IF(KEND.GE.KENDF)GO TO 202
      I=11
      V1=V10
      V=V10
      IV=1
      ILL=1
      IEOF=0
      SUM=0.0
      VBOT=V1-A-BOUND
      VTOP=V2+A+BOUND
      GO TO 11
202  CONTINUE
      REWIND 2
      IF(IRUN.LT.6)GO TO 1015
      CALL EXIT
C
77  FORMAT (E12.5,F7.2)
81  FORMAT (7E10.3)
85  FORMAT (6F10.3)
79  FORMAT (' PRESSURE =',E12.5,'TEMPERATURE =',F7.2)
83  FORMAT (3X,'WATER',6X,'CO2',6X,'OZONE',7X,'N2O',7X,'CO',8X,'CH4',7
      1X,'O2',4X)
87  FORMAT (' V1 =',F10.3,'V2 =',F10.3,'DV=',F10.3,'BOUND =',F10.3,'A
      1=',F10.3,'DELV =',F10.3)
89  FORMAT (' PARITY ERROR ENCOUNTERED AT',F12.3)
91  FORMAT (' END OF FILE ENCOUNTERED',15)
97  FORMAT (' VBOT =',F12.3,'VTOP =',F12.3,'GNU =',F12.3,'11 ',18)
103 FORMAT ('JFNU =',15)
104 FORMAT (5(' FREQUENCY TRANS. '))
93  FORMAT (110)
95  FORMAT (F10.3,E10.3,F5.3,F10.3,35X,13,14,13)
101 FORMAT (15,2F10.4)
105 FORMAT (5(F10.3,E12.5))
      STOP
      END

```

OF COMPILATION:

NO DIAGNOSTICS.



APPENDIX 3

Part 1 of Slant Path Program



```

862 FORMAT(7F10.5)
   TQV(1)=175.
   DO 863 I=2,7
863  TQV(I)=TQV(I-1)+25.
   TQV(6)=296.

C
C   READ INPUT PARAMETERS (P=PRESSURE), (T=TEMPERATURE),
C   W(1)=H2O, W(2)=CO2, W(3)=O3, W(4)=N2O, W(5)=CO, W(6)=CH4, W(7)=O2.
C   V1 AND V2 ARE FREQUENCY LIMITS FOR WHICH OUTPUT RESULTS ARE REQUIRED.
C   DV IS MONOCHROMATIC FREQUENCY INCREMENT.
C   BOUND IS THE FREQUENCY FROM ANY LINE CENTER BEYOND WHICH THE LINE
C   WILL BE NEGLECTED.
C   A IS THE HALF-WIDTH OF A TRIANGULAR S1IT FUNCTION.
C   DELV IS FREQUENCY INCREMENT OF CONVOLVED OUTPUT TRANSMITTANCE
C   RESULTS.
C
C   FOR CO2 FILTERS NOAA OR DAP, V1=605.0, V2=767.0, DV=.001, DELV=.01
C   BOUND=15.0, A=.005
C
   READ(5,896)NW,SMIN
896  FORMAT(15,E10.3)
   READ(5,85)V1,V2,DV,BOUND,A,DELV
   DELVX=1.0D-2
   DELV=DELVX
   AX=5.0D-3
   A=AX
   DVX=1.0D-3
   DV=DVX
   V1X=V1
   V10=V1X
   V20=V2
   PRINT 87,V1,V2,DV,BOUND,A,DELV
C   IF(A*2/DV+1.GT.3000) CALCULATION CANNOT BE DONE
C   IF THERE ARE MORE THAN 3000 LINES READ FROM TAPE IN A FREQUENCY RANGE
C   OF 2(A+BOUND) CALCULATION CANNOT BE DONE
   VBOT=V1-A-BOUND
   VTOP=V2+A+BOUND
   I=1
   ILL=1
   REWIND 2
   IREAD=0
1   READ(2,95)GNU(I),S(I),ALPHA(I),EDP(I),IDAT,ISOT,NO
   IF(GNU(I).LT.VBOT)GO TO 1
   IF(GNU(I).GT.VTOP)GO TO 11
   IF(MO.NE.NW)GO TO 1
   IF(S(I).LT.SMIN)GO TO 1
   IF(EDP(I).LT.500.)GO TO 850
   IF(S(I).GT.1.0E-23) GO TO 850
   IF(EDP(I).LT.1000.0.AND.S(I).GT.1.0E-24)GO TO 850
   IF(GNU(I).GT.720..AND.S(I).GT.1.0E-25)GO TO 850
   GO TO 1
850  CONTINUE
   IF(I.GT.2999)GO TO 11
   I=I+1
   GO TO 1
11   I1=I

```

```

      MO=NW
204 CONTINUE
      PRINT 97, VBOT, VTOP, GNU(I1), I1
      IS=1
      V2P=GNU(I1)-BOUND-A
      IF (V2P.LT.V2) GO TO 870

C
C   TAPE HAS BEEN READ FOR ALL NECESSARY LINES OR FOR THE MAXIMUM NO.
C   OF LINES POSSIBLE SUBJECT TO RECYCLING.
C   HALFWIDTHS WILL BE SUPPLIED BELOW WHEN THEY DO NOT APPEAR
C   ON TAPE.
C
      DO 15 I=ILL, I1
      M=NW
      IF (M.EQ.1) GO TO 15
      IF (ALPHA(I).GT.0.0) GO TO 13
      IF (M.EQ.2) ALPHA(I)=0.07
      IF (M.EQ.3) ALPHA(I)=0.11
      IF (M.EQ.4) ALPHA(I)=0.08
      IF (M.EQ.5) ALPHA(I)=0.06
      IF (M.EQ.6) ALPHA(I)=0.055
      IF (M.EQ.7) ALPHA(I)=0.048
13    IF (ALPHA(I).LT.0.01.OR.ALPHA(I).GT.1.0) ALPHA(I)=0.06
15    CONTINUE

C
C   READ LAYER DATA
876 CONTINUE
      DO 780 M=1, 1000
      TRANS(M)=0.0
      READ(5, 777) P1, T1, P2, T2
      777 FORMAT(2(E12.5, F7.2))
      P=(P1+P2)/2.
      T=(T1+T2)/2.
      PRINT 789, P1, P2, P, T1, T2, T
      789 FORMAT(2X, 'P1=', F7.2, 'P2=', F7.2, 'PAV=', F7.2, 'T1=', F6.2, 'T2=', F6.2,
1    'TAV=', F6.2)
      DP=P2-P1
      READ(5, 81) (W(M), M=1, 7)
      PRINT 83
      PRINT 81, (W(M), M=1, 7)
      PRINT 700, (W(M), M=1, 7)
      700 FORMAT(14H W IN MOL/CM2, 7(2X, E12.6))
C
C   MODIFY BOUND FOR PRESSURE. LE. 3.5*P
C
      BOUND=.014*P
      IF (BOUND.LT.0.005) BOUND=0.005
      MIN=0
      DO 870 M=2, 7
      MIN=MIN+1
      IF (T.LE.TQV(M)) GO TO 871
      870 CONTINUE
      871 QV=(T-TQV(MIN))/(TQV(MIN+1)-TQV(MIN),
      DO 869 M=1, 7
      869 QV(M)=(QV(M, MIN)+(QV(M, MIN+1)-QV(M, MIN)))/QV(M, 6)
      WRITE(8, 874)
      874 FORMAT('FOR LAYER NUMBER')

```



AD-A069 041

TEXAS UNIV AT EL PASO DEPT OF ELECTRICAL ENGINEERING  
ATMOSPHERIC TRANSMITTANCE STUDY WITH THE METEOROLOGICAL SATELLI--ETC(U)  
OCT 76 R E BRUCE, J H PIERLUISSI, S K WEAVER DAEA18-76-C-0019  
PR4-76-DC-30-PT-2 NL

UNCLASSIFIED

2 OF 2  
AD  
AO-8041



END  
DATE  
FILMED  
7-79  
DDC

```

WRITE(R,872)ILA
WRITE(R,107)
107 FORMAT('HOMOGENEOUS PATH OUTPUT FOR GASES AS FOLLOWS' )
WRITE(R,81) (MIN),M=1,7)
WRITE(R,85)V1,V2,DV,BOUND,A,DELV
WRITE(R,779)P1,P2,P,I1,I2,I
779 FORMAT(6(2X,F7.2))
X=(V2-V1)/DELV+0.1
NX=(X+1.0)
WRITE(R,108)NX
108 FORMAT(' NUMBER OF DATA POINTS =',I10)
IS=1
P0=1013.00
T0=296.00
CS1=(T0-T)/(T0*T*0.6946)
C
C ROTATIONAL PARTITION FUNCTION IS DEFINED BELOW
C
DO 21 M=1,7
IF (M.EQ.1) GO TO 17
IF (M.EQ.2) GO TO 19
IF (M.EQ.3) GO TO 17
IF (M.EQ.4) GO TO 19
IF (M.EQ.5) GO TO 19
IF (M.EQ.6) GO TO 17
IF (M.EQ.7) GO TO 19
17 CS2(M)=((T0/T)**1.5)
GO TO 21
19 CS2(M)=T0/T
21 CONTINUE
CA=((T0/T)**0.5)*(P/P0)
CAX=CA/CA0
DO 882 I=1,I1
882 ALPHA(I)=ALPHA(I)*CAX
CA0=CA
C * SETUP XL(I)
DO 883 I=1,I1
883 XL(I)=S(I)*CS2(NW)*QVF(NW)*EXP(-EDP(I)*CS1)
C
C TEMPERATURE DEPENDENCE OF ALL LINE INTENSITIES COMPUTED HERE.
C
VX=VIX-AX
V=VX
25 CAY=0.0
C
C DETERMINE INDICES (15 AND 16) INDICATING WHICH SPECTRAL LINES
C ARE TO BE USED IN CALCULATIONS AT FREQUENCY V.
C
DO 33 I=15,I1
IF (V-BOUND-GNU(I)) 29,29,33
29 IS=I
GO TO 35
33 CONTINUE
IS=11
GO TO 49
35 DO 39 J=15,I1

```

```

      IF (V+BOUND-GNU(J)) 37,37,39
37   I6=J-1
      GO TO 43
39   CONTINUE
      I6=I1
C
C   COMPUTE THE OPTICAL DEPTH AND TRANSMITTANCE AT FREQUENCY V.
C   C USES LORENTZ LINE ONLY
C
43   DO 45 I=I5,I6
      Z=ABS(V-GNU(I))
      IF (Z.GT.BOUND) GO TO 851
      SUMI=XI(I)*ALPHA(I)/(Z*Z+ALPHA(I)*ALPHA(I))
      GO TO 852
851  SUMI=0.
852  CAY=CAY+SUMI
45   CONTINUE
      OPD(IV)=CAY*0.3183*W(NW)*DP
      GO TO 51
49   OPD(IV)=0.0
51   OPD(IV)=EXP(-OPD(IV))
339  CONTINUE
      IF ((IV+DV).GT.V2P) GO TO 53
      IF (V.GE.V2+A) GO TO 53
      IF (IV.GE.3000) GO TO 53
      IV=IV+1
      VX=VX+DVX
      V=VX
      GO TO 25
C
C   AT THIS POINT, CYCLE BACK TO STATEMENT 25 AND COMPUTE THE
C   MONOCHROMATIC TRANSMITTANCE AT V+DV,ETC.
C   IF STATEMENT 53 IS REACHED ,ALL POSSIBLE MONOCHROMATIC TRANSMITTANCE
C   VALUES HAVE BEEN COMPUTED, AND THE SLIT FUNCTION CONVOLUTION WILL
C   NOW BE PERFORMED IN LOOP 57
C
53   FREQ=V1
      FREQX=VIX
      FREQ=FREQX
      PRINT 101, IV,V,V2P
C   WRITE OUT TRANSMISSIONS, MONOCHROMATIC
201  FORMAT(10F12.8)
      XD=3.0D+3*DVX-AX-DELVX
      FINALX=VIX+XD
      FINAL =FINALX
      VX=VIX-AX
      V=VX
      JFNU=1
      L=DELV/DV+0.01
      IA=1
55   SUM=0.0
      SUMI=0.0
      DO 57 I=IA,IV
      SUM=SUM+OPD(I)
      SUMI=SUMI+1.0
      VX=VX+DVX

```

```

V=VX
IF (V-(FREQ+A)) 57,59,59
57 CONTINUE
59 TRANS(JFNU)=SUM/SUM1
FNU(JFNU)=FREQ
IF (FREQ.GT.V2) GO TO 61
IF (FREQ.GE.FINAL) GO TO 61
FREQX=FREQX+DEL VX
FREQ=FREQX
IF (JFNU.GE.1000) GO TO 61
JFNU=JFNU+1
IA=IA+L
VX=FREQX-AX
V=VX
SUM=0.0
GO TO 55

C
C CONVOLVED TRANSMITTANCE RESULTS ARE NOW PRINTED OUT.
C
61 PRINT 103, JFNU
PRINT 104
PRINT 105, (FNU(J),TRANS(J),J=1,JFNU)
WRITE(8,109) JFNU
109 FORMAT(15)
WRITE(8)TRANS
106 FORMAT(6E12.6)
IF (FREQ.GE.V2) GO TO 75
IF (JFNU.GE.1000) GO TO 65
IF (FREQ.GE.FINAL) GO TO 63
GO TO 75
63 VIX=FREQX+DEL VX
V1=VIX
IS=1
IV=1
JFNU=1
VX=VIX-AX
V=VX
GO TO 25
65 IA=IA+L

C
C IF STATEMENT 65 IS REACHED, ADDITIONAL MONOCHROMATIC CALCULATIONS
C ARE REQUIRED TO SATISFY THE TOTAL FREQUENCY RANGE OVER WHICH
C CONVOLVED RESULTS ARE REQUIRED.
C
JFNU=1
VX=FREQX-AX
V=VX
GO TO 55
75 CONTINUE
JFNU=0
WRITE(8,109) JFNU
ILA=ILA+1
JFNU=1
IS=1
IV=1
VIX=V10

```



```

V1=V10
V2=V20
IF(ILA.GT.ILAY) GO TO 875
GO TO 876
875 CONTINUE
REWIND 8
REWIND 2
READ(8,110) (SYMB(I),I=1,3)
WRITE(6,110) (SYMB(I),I=1,3)
READ(8,110) (SYMB(I),I=1,7)
WRITE(6,110) (SYMB(I),I=1,7)
READ(8,872) ILAY
877 CONTINUE
READ(8,110) (SYMB(I),I=1,3)
READ(8,872) ILA
READ(8,110) (SYMB(I),I=1,8)
110 FORMAT(7A6,A2)
WRITE(6,110) (SYMB(I),I=1,8)
WRITE(6,83)
READ(8,81) (W(M),M=1,7)
WRITE(6,81) (W(M),M=1,7)
READ(8,85) V1,V2,DV,BOUND,A,DELV
WRITE(6,87) V1,V2,DV,BOUND,A,DELV
READ(8,779) P1,P2,P,T1,T2,T
WRITE(6,789) P1,P2,P,T1,T2,T
READ(8,108) NX
WRITE(6,108) NX
500 READ(8,109) JFNU
WRITE(6,109) JFNU
IF(JFNU.EQ.0) GO TO 502
IF(JFNU.LE.NX) GO TO 501
WRITE(6,112)
503 CONTINUE
112 FORMAT(' JFNU GT NX ')
501 READ(8) TRANS
WRITE(6,106) (TRANS(J),J=1,JFNU)
NX=NX-JFNU
IF(NX.GT.1) GO TO 500
READ(8,109) JFNU
IF(JFNU.NE.0) GO TO 503
502 CONTINUE
IF(ILA.GE.ILAY) GO TO 878
GO TO 877
890 WRITE(6,891)
891 FORMAT(' V2P GREATER THAN V2 - ERROR STOP')
878 CONTINUE
REWIND 8
202 CALL EXIT

```

```

C
77 FORMAT (E12.5,F7.2)
81 FORMAT (7E10.3)
85 FORMAT (6F10.3)
79 FORMAT (' PRESSURE =',E12.5,' TEMPERATURE =',F7.2)
83 FORMAT (3X,'WATER',6X,'CO2',6X,'OZONE',7X,'N2O',7X,'CO',8X,'CH4',7
1X,'O2',4X)
87 FORMAT (' V1 =',F10.3,' V2 =',F10.3,' DV=',F10.3,' BOUND =',F10.3,' A

```

```

1=,F10.3,'DELV =',F10.3)
89  FORMAT (' PARITY ERROR ENCOUNTERED AT',F12.3)
91  FORMAT (' END OF FILE ENCOUNTERED',15)
97  FORMAT (' VBOT =',F12.3,'VTOP =',F12.3,'GNU =',F12.3,'11 ',18)
103 FORMAT ('JFNU =',15)
104 FORMAT (5(' FREQUENCY      TRANS.      '))
93  FORMAT (110)
95  FORMAT (F10.3,E10.3,F5.3,F10.3,35X,13,14,13)
101 FORMAT (15,2F10.4)
105 FORMAT (5(F10.3,E12.5))
STOP
END

```

QXQT

37

1.0	1.0	1.0	1.0	1.0	1.0	1.001
1.0095	1.0192	1.0327	1.0502	1.0719	1.0931	1.1269
1.004	1.007	1.013	1.022	1.033	1.046	1.066
1.017	1.03	1.048	1.072	1.1	1.127	1.17
1.0	1.0	1.0	1.0	1.0	1.0	1.0
1.0	1.0	1.001	1.002	1.004	1.007	1.011
1.0	1.0	1.0	1.0	1.0	1.0	1.001

2+1.000E-25

650.	670.	.001	15.	.005	.01
+ .160 E-02	180.65	.100 E-01	180.65		
.0 E 0 6.785E+18	.0 E 0	.0 E 0	.0 E 0	.0 E 0	.0 E 0
.100 E-01	180.65	.40 E-01	210.22		
.0 E 0 6.785E+18	.0 E 0	.0 E 0	.0 E 0	.0 E 0	.0 E 0
.400 E-01	210.22	.70 E-01	225.97		
.0 E 0 6.785E+18	.0 E 0	.0 E 0	.0 E 0	.0 E 0	.0 E 0
.700 E-01	225.97	.10 E 00	235.65		
.0 E 0 6.785E+18	.0 E 0	.0 E 0	.0 E 0	.0 E 0	.0 E 0
.100 E 00	235.65	.40 E 00	264.15		
.0 E 0 6.785E+18	.0 E 0	.0 E 0	.0 E 0	.0 E 0	.0 E 0
.400 E 00	264.15	.70 E 00	270.65		
.0 E 0 6.785E+18	.0 E 0	.0 E 0	.0 E 0	.0 E 0	.0 E 0
.700 E 00	270.65	.10 E+01	270.65		
.0 E 0 6.785E+18	.0 E 0	.0 E 0	.0 E 0	.0 E 0	.0 E 0
.100 E+01	270.65	.13 E+01	267.17		
.0 E 0 6.785E+18	.0 E 0	.0 E 0	.0 E 0	.0 E 0	.0 E 0
.130 E+01	267.17	.16 E+01	262.51		
.0 E 0 6.785E+18	.0 E 0	.0 E 0	.0 E 0	.0 E 0	.0 E 0
.160 E+01	262.51	.20 E+01	257.87		
.0 E 0 6.785E+18	.0 E 0	.0 E 0	.0 E 0	.0 E 0	.0 E 0
.20 E+01	257.87	.25 E+01	253.20		
.0 E 0 6.785E+18	.0 E 0	.0 E 0	.0 E 0	.0 E 0	.0 E 0
.25 E+01	253.20	.30 E+01	249.38		
.0 E 0 6.785E+18	.0 E 0	.0 E 0	.0 E 0	.0 E 0	.0 E 0
.30 E+01	249.38	.40 E+01	243.65		
.0 E 0 6.785E+18	.0 E 0	.0 E 0	.0 E 0	.0 E 0	.0 E 0
.40 E+01	243.65	.50 E+01	239.27		
.0 E 0 6.785E+18	.0 E 0	.0 E 0	.0 E 0	.0 E 0	.0 E 0
.50 E+01	239.27	.65 E+01	234.09		
.0 E 0 6.785E+18	.0 E 0	.0 E 0	.0 E 0	.0 E 0	.0 E 0
.65 E+01	234.09	.80 E+01	230.06		
.0 E 0 6.785E+18	.0 E 0	.0 E 0	.0 E 0	.0 E 0	.0 E 0
.80 E+01	230.06	.10 E+02	227.06		

.0	E	0	6.785E+18	.0	E	0	.0	E	0	.0	E	0	.0	E	0	.0	E	0
.10	E+02	227.06		.13	E+02	225.95												
.0	E	0	6.785E+18	.0	E	0	.0	E	0	.0	E	0	.0	E	0	.0	E	0
.13	E+02	225.95		.16	E+02	224.59												
.0	E	0	6.785E+18	.0	E	0	.0	E	0	.0	E	0	.0	E	0	.0	E	0
.16	E+02	224.59		.20	E+02	223.12												
.0	E	0	6.785E+18	.0	E	0	.0	E	0	.0	E	0	.0	E	0	.0	E	0
.20	E+02	223.12		.25	E+02	221.67												
.0	E	0	6.785E+18	.0	E	0	.0	E	0	.0	E	0	.0	E	0	.0	E	0
.25	E+02	221.67		.30	E+02	220.50												
.0	E	0	6.785E+18	.0	E	0	.0	E	0	.0	E	0	.0	E	0	.0	E	0
.30	E+02	220.50		.40	E+02	218.65												
.0	E	0	6.785E+18	.0	E	0	.0	E	0	.0	E	0	.0	E	0	.0	E	0
.40	E+02	218.65		.50	E+02	217.22												
.0	E	0	6.785E+18	.0	E	0	.0	E	0	.0	E	0	.0	E	0	.0	E	0
.50	E+02	217.22		.65	E+02	216.65												
.0	E	0	6.785E+18	.0	E	0	.0	E	0	.0	E	0	.0	E	0	.0	E	0
.65	E+02	216.65		.80	E+02	216.65												
.0	E	0	6.785E+18	.0	E	0	.0	E	0	.0	E	0	.0	E	0	.0	E	0
.80	E+02	216.65		.10	E+03	216.65												
.0	E	0	6.785E+18	.0	E	0	.0	E	0	.0	E	0	.0	E	0	.0	E	0
.10	E+03	216.65		.13	E+03	216.65												
.0	E	0	6.785E+18	.0	E	0	.0	E	0	.0	E	0	.0	E	0	.0	E	0
.13	E+03	216.65		.16	E+03	216.65												
.0	E	0	6.785E+18	.0	E	0	.0	E	0	.0	E	0	.0	E	0	.0	E	0
.16	E+03	216.65		.20	E+03	216.65												
.0	E	0	6.785E+18	.0	E	0	.0	E	0	.0	E	0	.0	E	0	.0	E	0
.20	E+03	216.65		.25	E+03	220.87												
.0	E	0	6.785E+18	.0	E	0	.0	E	0	.0	E	0	.0	E	0	.0	E	0
.25	E+03	220.87		.30	E+03	228.67												
.0	E	0	6.785E+18	.0	E	0	.0	E	0	.0	E	0	.0	E	0	.0	E	0
.30	E+03	228.67		.40	E+03	241.46												
.0	E	0	6.785E+18	.0	E	0	.0	E	0	.0	E	0	.0	E	0	.0	E	0
.40	E+03	241.46		.50	E+03	251.90												
.0	E	0	6.785E+18	.0	E	0	.0	E	0	.0	E	0	.0	E	0	.0	E	0
.50	E+03	251.90		.65	E+03	264.84												
.0	E	0	6.785E+18	.0	E	0	.0	E	0	.0	E	0	.0	E	0	.0	E	0
.65	E+03	264.84		.80	E+03	275.48												
.0	E	0	6.785E+18	.0	E	0	.0	E	0	.0	E	0	.0	E	0	.0	E	0
.80	E+03	275.48		.10	E+04	287.50												
.0	E	0	6.785E+18	.0	E	0	.0	E	0	.0	E	0	.0	E	0	.0	E	0

08007\*CHECK.MONITOR,E  
0FIN